

Chapter 2

System Noise Concepts with DSN Applications

Charles T. Stelzried, Arthur J. Freiley, and Macgregor S. Reid

2.1 Introduction

The National Aeronautics and Space Administration/Jet Propulsion Laboratory (NASA/JPL) Deep Space Network (DSN) has been evolving toward higher operational frequencies for improved receiving performance for the NASA deep space exploration of our Solar System. S-band (2.29–2.30 gigahertz [GHz]), X-band (8.40–8.50 GHz), and Ka-band (31.8–32.3 GHz) are the 2006 deep space downlink (ground receive) frequency bands. These internationally allocated microwave downlink frequency bands are listed in Table 2-1. The DSN is considering the use of higher microwave frequencies as well as optical frequencies for the future. Higher frequencies generally provide improved link performance, thus allowing higher data rates.

The communications link performance is critically dependent upon the receiving system antenna gain (proportional to antenna area) and the noise temperature performance; a system figure of merit of gain-to-temperature ratio (G/T) is defined in Section 2.5.1. This chapter provides the definitions and calibration techniques for measurements of the low noise receiving systems. Noise in a receiving system is defined as an undesirable disturbance corrupting the information content. The sources of noise can be separated into external and internal noise. Sources of external noise [1–5] include Cosmic Microwave Background (CMB), Cosmic Microwave Foreground (CMF), galactic and radio sources, solar, lunar, and planetary sources, atmospheric (includes lightning), atmospheric absorption, man-made noise, and unwanted antenna pickup. The

Table 2-1. 2006 DSN allocated operational deep space downlink microwave frequencies.

DSN Microwave Band	Mid-Band Frequencies (GHz)	Allocated Frequencies (GHz)
S	2.295	2.29–2.30
X	8.425	8.40–8.45
Ka	32.05	31.8–32.3

CMB noise [6] is considered to be the residual radiation, currently measured to be 2.725 K, [7] from the origin of the universe (Big Bang). CMF noise includes emission from diffuse Galactic and unresolved point sources [8] collected by the antenna. Man-made noise or radio frequency interference (RFI) includes coherent signal generation as well as ignition systems, spark discharges, and transmission of noise signals emanating from power transmission lines. The CMF contribution is small compared to the CMB for DSN applications. The CMB and the atmosphere are the dominant external noise sources for the DSN microwave receiving systems.

Sources of internal noise include [9, 10, and 4 (p. 4)] thermal, shot, current, and Barkhausen noise. Thermal noise is the minimum internal noise source for microwave receiving systems. The noise performance of DSN low-noise amplifiers (LNAs) is typically expressed in terms of noise temperature (Section 2.2.6). For example, LNAs with a noise figure range of 1.010 to 1.014 (ratio) are more conveniently characterized with a noise temperature range of 3 to 4 kelvins.

Thin sheet Kapton at the feedhorn apertures retains the nitrogen pressure in the feedhorns and associated waveguide components. On the 70-meter (70-m) tricorne-equipped antennas, blowers are installed at the X-band feedhorn aperture in an attempt to reduce signal attenuation and increased noise contribution due to rain or dew effects on the horn covers. Rain adhering to the weathered Kapton feedhorn cover causes measurable degradation effects at all DSN frequencies, including S-band. An important strategy is to maintain fresh Kapton horn covers to minimize the degradation. These precautions are not necessary with the DSN 34-m beam waveguide (BWG) antennas since the feedhorns are not exposed to weather.

In this chapter, system noise temperature contributions and measurement techniques are presented and analyzed for typical receiving systems of the DSN. The antenna, LNA, and receiver assemblies comprise the receiving system. The DSN adheres to the Institute of Electrical and Electronics Engineers (IEEE) noise temperature definitions [11,12]. Mismatch effects are minimized with the use of matched components in the LNA input configuration [13].

The large antennas of the DSN required for deep space communications are described in [14,15] and Chapter 1 of this book. The 70-m antennas are the

largest and most powerful in the DSN with three [16] Cassegrain feedcones ('tricone') shown in Fig. 2-1. The X-band transmit receive (XTR) feedcone has a high-pass dichroic frequency selective reflector (i.e., it passes X-band and reflects S-band), shown in the retracted position (Fig. 2-2) for X-band only



Fig. 2-1. Goldstone 70-m antenna tricones S-band polarization diversity (SPD) feedcone located behind the X-band/K-band radar (XKR) and X-band transmit/receive (XTR) feedcone.

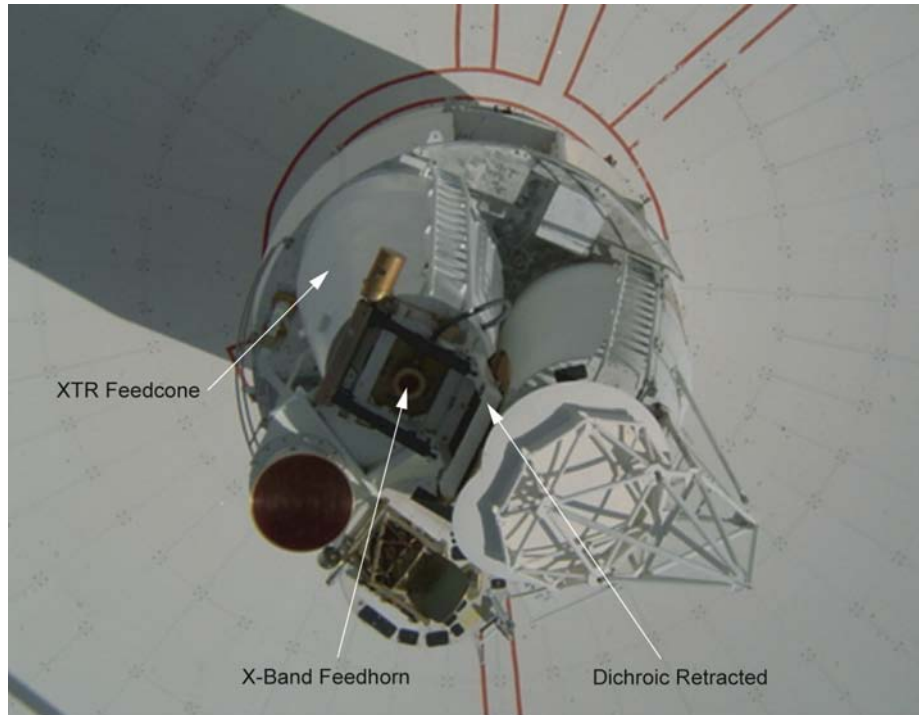


Fig. 2-2. Goldstone 70-m antenna tricones showing XTR feedcone with S-band/X-band dichroic retracted as viewed from the subreflector.

operations. This reflector is moved to the extended position (Fig. 2-3) for simultaneous S-X-band operation. Thus, by means of two relatively small (sub-sub) reflectors, simultaneous use of two of the three feedcones is obtained, with nearly coincident beam (co-axial S-X beam) pointing and essentially no beam scan loss. This XTR feedcone configuration is used in Section 2.5 as an example of DSN noise temperature system calibration. These noise temperature calibrations of the LNA with a standard calibrated zenith pointing feedhorn (test a), a completed feedcone assembly in a ground zenith configuration (test b) and the completed system on the antenna (test c) results in a fully calibrated system. The system noise temperatures of the operational systems are verified with routine periodic measurements.

The system operating noise temperature (T_{op}) for a DSN receiving system is measured by switching the LNA between a calibration ambient load and the antenna. T_{op} arises from multiple contributions defined at the feedhorn aperture.

$$T_{op} = T_{sky} + T_{ant} + T_{feed} + T_{LNA} + T_f \quad (2.1-1)$$

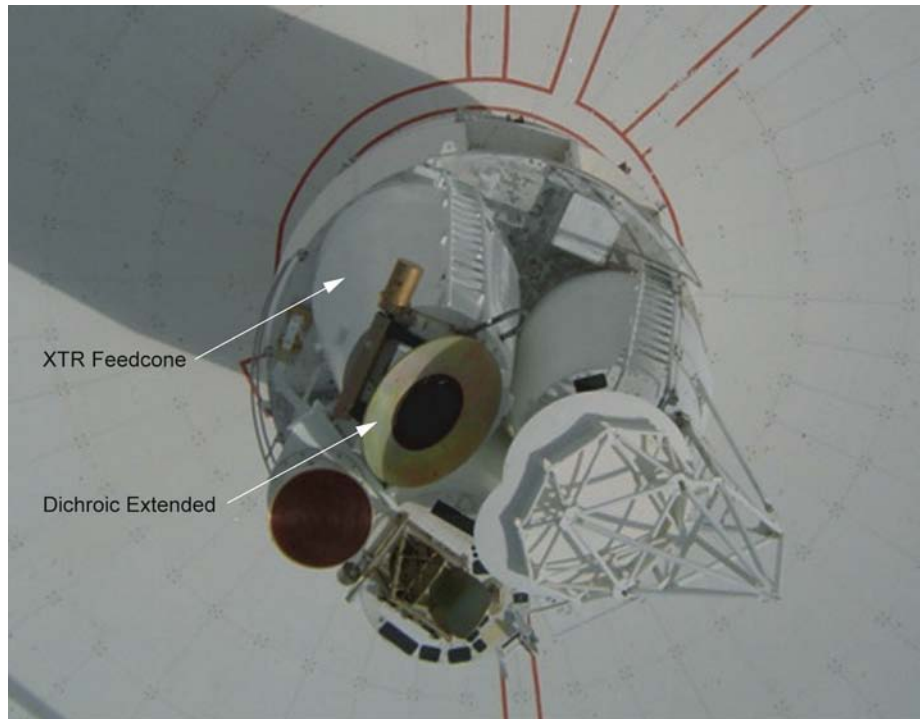


Fig. 2-3. Goldstone 70-m antenna tricones showing XTR feedcone with S-band/X-band dichroic extended as viewed from the subreflector.

T_{op} is composed of the sky noise temperature and the ground antenna and microwave system

$$T_{op} = T_{sky} + T_{AMW} \quad (2.1-2)$$

where

T_{op} system operating noise temperature, K

$T_{sky} = T_{atm} + T_{CMB} / L_{atm}$ = combined noise temperature contribution of T_{atm} and T_{CMB} , K

T_{CMB} = CMB noise temperature, K

T_{atm} = noise temperature contribution due to the atmosphere, K

L_{atm} = atmospheric loss, ratio

T_{ant} = noise temperature contribution due to the antenna, K

T_{feed} = noise temperature of the microwave feed components, K

T_{LNA} = LNA noise temperature, K

T_f = follow-up amplifier noise temperature, K

$T_{\text{AMW}} = T_{\text{ant}} + T_{\text{feed}} + T_{\text{LNA}} + T_f =$ antenna microwave system
effective input noise temperature, K

2.2 Noise Temperature Concepts

2.2.1 Thermal Noise

The concept of thermal noise is stated by W. Mumford [4 (p. 3)] as: “The random motion of the free electrons in a conductor caused by thermal agitation gives rise to a voltage at the open ends of the conductor. In most conductors, the frequency components of this noise cover the whole radio spectrum uniformly.”

Thermal or Johnson [9] noise power density available from a source such as an antenna or a resistive termination (load) is given by [11 (p. 735)]

$$N = k T_p \quad (2.2-1)$$

where

N = noise power density, W/Hz

k = Boltzmann’s constant = 1.38065×10^{-23} , J/K

T_p = resistive termination physical temperature, K

A reduction of noise power at higher frequencies according to Planck’s radiation law is ignored for present DSN applications. Accurate system operating noise temperature results (as analyzed and verified in Section 2.2.3) are obtained without application of Planck’s radiation law noise temperature reduction. This simplifies the analysis and calculations, and is in accordance with IEEE standards [11 (p. 734)].

Connecting a resistive source to the input of a noiseless amplifier (with available power gain G and noise bandwidth B) provides amplifier output noise power N_o [4 (p. 12)]

$$N_o = k T_p B G \quad (2.2-2)$$

where

N_o = amplifier output noise power with resistive source and noiseless amplifier, W

$B = (1 / G_m) \int G(f) df =$ noise bandwidth [4 (p. 13)], Hz

f = operating frequency, Hz

$G = G(f)$ = available power gain, ratio

G_m = maximum available power gain [4 (p. 8)], ratio

k = Boltzmann's constant = 1.38065×10^{-23} , J/K

T_p = resistive termination physical temperature, K

The standard ambient noise temperature is $T_o = 290$ K, which from Eq. 2.2-1 gives an available noise power of -203.975 dB relative to 1 W/Hz-K. Similarly, $T = 1$ K results in a noise power of -228.599 dB relative to 1 W/Hz-K (or -198.6 dBm relative to 1 mw/Hz-K).

2.2.2 System Operating Noise Temperature

The preceding discussion and definitions lead to a system operating noise temperature concept. System operating noise temperature is important for the DSN, and for other operational systems, for the determination of the operating communications system performance between the spacecraft and the ground antennas. Although this discussion focuses on the downlink analysis, the concepts apply to the uplink analysis as well.

Consistent with Eq. (2.2-2), and Fig. 2-4, system operating noise temperature (T_{op}) is given by [4 (p. 34)]

$$T_{op} = \frac{P_o}{kBG} \quad (2.2-3)$$

where

T_{op} = system operating noise temperature, K

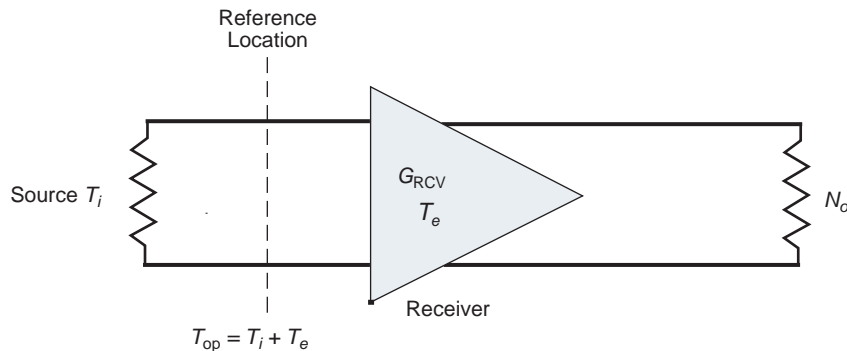


Fig. 2-4. Receiving system consisting of an input source (typically an antenna or ambient resistive load) and an amplifier with a single reference location for defining the system noise temperature, T_{op} , in terms of T_i and T_e .

P_o = receiver output noise power, W

T_{op} is always defined for a specific reference location as shown in Fig. 2-4. T_{op} is composed of both an incident input noise temperature and the receiver effective input noise temperature [11 (p. 766)].

$$T_{op} = T_i + T_e \quad (2.2-4)$$

where

T_{op} = system operating noise temperature, K

T_i = input source noise temperature, K

T_e = receiver effective input noise temperature, K

2.2.3 Planck's Radiation Law Noise Power Reduction

The purpose of this section is to evaluate Planck's radiation law noise power reduction at higher frequencies on measurements of system noise temperature T_{op} . The correction for T_{op} that results from the reduced noise power is analyzed for a range of frequencies and temperatures. For microwave frequencies below 100 GHz, this correction is not necessary, nor is it used for DSN calibrations [18].

The noise temperature reduction for a resistive calibration termination as a function of frequency is shown in Fig. 2-5 using Planck's radiation law noise power reduction [4 (p. 76)] is given by

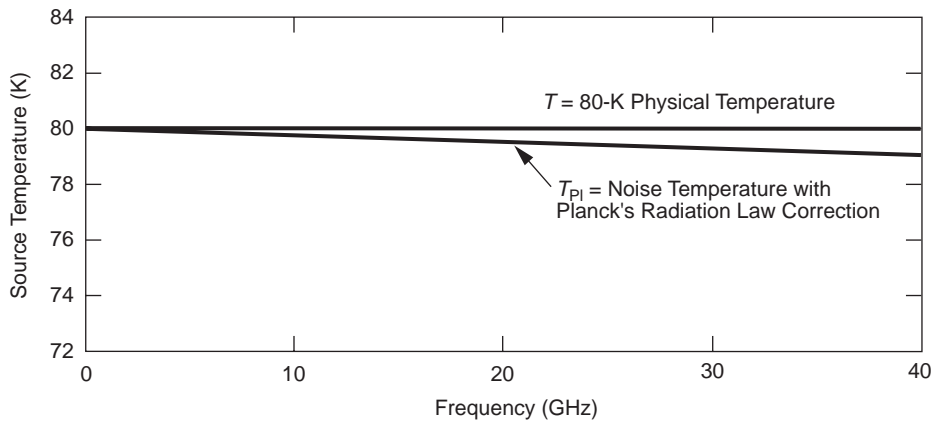


Fig. 2-5. Source noise temperature at a physical temperature of 80 K (horizontal line) and showing Planck's radiation law noise temperature reduction versus frequency.

$$T_{Pl} = T \left[\frac{x}{e^x - 1} \right] \quad (2.2-5)$$

where

T_{Pl} = source noise temperature with Planck's radiation law correction,
K

T = source physical temperature, K

h = Planck's constant = 6.626069×10^{-34} , Js

f = frequency, Hz (unless noted otherwise)

$x = hf/kT \sim 0.048 f(\text{GHz})/T(\text{K})$, ratio

From Eq. (2.2-5) at 32 GHz, Planck's radiation law reduces the noise temperature of a resistive termination with a physical temperature of 80 K by 0.765421 K. However, an accurate system temperature measurement results without the Planck's correction as shown in the following equations. This results from a lower measured receiver effective input noise temperature, which nearly cancels the higher antenna noise temperature.

As discussed, and with terms defined in Section 2.6, a receiver effective input noise temperature calibration consists of measuring the 'Y-factor' power ratio by switching the receiver input between the cold and hot loads.

$$Y_{ch} = \frac{T_h + T_e}{T_c + T_e} \quad (2.2-6)$$

Solving for T_e in terms of the known cold and hot loads noise temperatures T_c and T_h

$$T_e = \frac{T_h - Y_{ch}T_c}{Y_{ch} - 1} \quad (2.2-7)$$

Also, system noise temperature, as discussed and defined in Section 2.6, can be determined by measuring the Y-factor power ratio by switching the receiver input between the hot load and the antenna

$$T_{Op} = \frac{T_h + T_e}{Y_{ah}} \quad (2.2-8)$$

Combining Eqs. (2.2-7) and (2.2-8)

$$T_{Op} = \frac{Y_{ch}(T_h - T_c)}{Y_{ah}(Y_{ch} - 1)} \quad (2.2-9)$$

using $Y = Y_{ch} / (Y_{ah} (Y_{ch} - 1))$, then

$$T_{op} = Y (T_h - T_c) \quad (2.2-10)$$

where

$$Y = Y_{ch} / [Y_{ah} (Y_{ch} - 1)], \text{ ratio}$$

$$Y_{ch} = P_h / P_c = \text{hot (ambient) and cold loads } Y\text{-factor, ratio}$$

$$Y_{ah} = P_h / P_a = \text{hot (ambient) load and antenna } Y\text{-factor, ratio}$$

The Y -factor ratio values are obtained from the calibration measurements and do not depend on whether or not it is planned to account for Planck's correction. The difference in T_{op} using the physical temperature of the loads versus Planck's correction is

$$\Delta T_{op, K} = T_{op} - T_{opPl} \quad (2.2-11)$$

$$\Delta T_{op, K} = Y [(T_h - T_c) - (T_h - T_c)_{Pl}] \quad (2.2-12)$$

$$\Delta T_{op, \%} = 100 \frac{(T_h - T_c) - (T_h - T_c)_{Pl}}{(T_h - T_c)} \quad (2.2-13)$$

where

$$(T_h - T_c) = \text{calibration loads physical temperatures difference, K}$$

$$(T_h - T_c)_{Pl} = \text{calibration load noise temperature difference with Planck's reductions, K}$$

Figure 2-6 shows a plot of ΔT_{op} as a percentage versus frequency. These curves are well behaved. The percentage difference in T_{op} due to using the load's physical temperatures versus Planck's reduction corrections for this example with 80-K and 290-K cold and hot calibration loads is only 0.00085 percent at 32 GHz. (The difference is larger at higher frequencies and lower cold load temperatures). The difference is less than 0.026 percent at 40 GHz with a 4-K cold load, the worst case shown for this range of parameters.

Expanding Planck's radiation law noise power reduction Eq. (2.2-5) [19 (p. 132)] in a Taylor series, assuming $x^2 < 4\pi^2$ where $x = hf/kT$

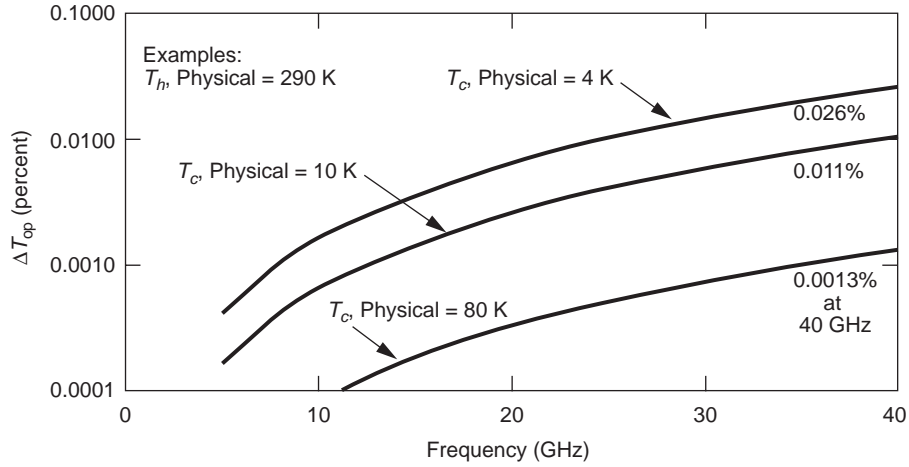


Fig. 2-6. System noise temperature measurement difference, ΔT_{op} in percent versus frequency, due to Planck's radiation law correction using a 290-K hot load and a range of cold load temperature.

$$T_{Pl} \approx T \left[1 - \left(\frac{x}{2} \right) + \left(\frac{x^2}{12} \right) + \dots \right] \quad (2.2-14)$$

$$T_{Pl} \approx T - \frac{\left(\frac{hf}{k} \right)}{2} + \frac{\left(\frac{hf}{k} \right)^2}{12T} + \dots \quad (2.2-15)$$

Using Eq. (2.2-13) with Eq. (2.2-15) ignoring higher order terms results in cancellation of the first two terms. This leaves only the third small term

$$\Delta T_{op}, \% \approx \frac{100 \left(\frac{hf}{k} \right)^2}{12T_c T_h} \quad (2.2-16)$$

Eq. (2.2-16) shows that the error ΔT_{op} (in percent) is increased at higher frequencies and lower calibration load temperatures. The value for ΔT_{op} (in percent) provides the error term for the system error analysis due to neglecting Planck's correction. For the DSN this error term is much smaller than the total errors due to other causes. At 32 GHz with $T_c = 80$ K and $T_h = 290$ K, Eq. (2.2-16) gives T_{op} (percentage = 0.00085) in agreement with the previous example with Eq. (2.2-13) and shown in Fig. 2-6.

The Planck correction with frequency is not needed for DSN operational microwave frequencies. The DSN reports measurements and analyses of system noise performance, at microwave frequencies, using the IEEE definition [11 (p. 735)] with the noise temperature of the calibration loads defined by their physical temperatures. This includes treating the CMB noise temperature as a constant 2.725 K over the range of DSN operational frequencies, all less than 100 GHz.

2.2.4 Translating Noise Temperature Reference Locations

System noise temperatures of a receiving system are defined for a specific reference location. Separate incident input and receiver effective noise temperatures are associated with the system noise temperature for that same given reference location. Typically, the individual noise temperature contributions are determined at other reference locations and must be translated to the common reference location. The equations for the various needed translations follow. It is assumed that the system is linear and that the components are ‘matched.’ For the three separate reference locations 1, 2, and 3 shown in Fig. 2-7, system noise temperatures by definition are

$$T_{op1} = T_{i1} + T_{e1} \quad (2.2-17)$$

$$T_{op2} = T_{i2} + T_{e2} \quad (2.2-18)$$

$$T_{op3} = T_{i3} + T_{e3} \quad (2.2-19)$$

T_i contains all the noise sources to the input side, and T_e contains all the noise sources to the output side of the reference location. With a component loss L (ratio, equal to or greater than 1) between the noise reference locations 1 and 2, and gain G (ratio, equal to or greater than 1) between the noise reference locations 2 and 3

$$T_{op1} = LT_{op2} \quad (2.2-20)$$

$$T_{op2} = \frac{T_{op1}}{L} \quad (2.2-21)$$

$$T_{op3} = GT_{op2} \quad (2.2-22)$$

G (ratio) and L (ratio) are always equal to or greater than 1, so that T_{op1} and T_{op3} are always equal to or greater than T_{op2} .

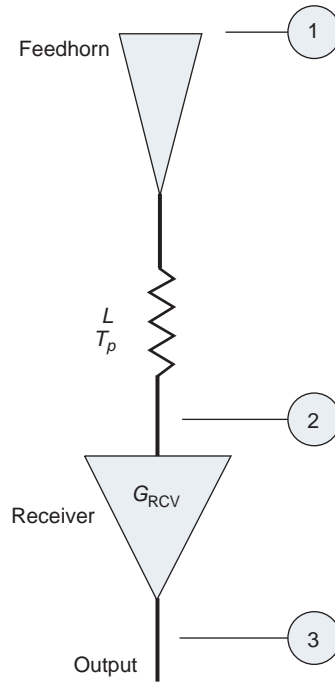


Fig. 2-7. Receiving system noise temperatures are defined at specific locations: Feedhorn aperture at reference location 1, receiver input at reference location 2, receiver output at reference location 3.

From Mumford [4 (p. 23)], the noise temperature translation equation between reference locations 1 and 2 separated by a loss L , ratio, with T_p , K equal to the physical temperature of the loss

$$T_{e1} = LT_{e2} + (L-1)T_p \quad (2.2-23)$$

Solving for T_{e2}

$$T_{e2} = \frac{T_{e1}}{L} - \left(1 - \frac{1}{L}\right)T_p \quad (2.2-24)$$

With Eqs. (2.2-4, -20, and -23)

$$T_{i1} = LT_{i2} - (L-1)T_p \quad (2.2-25)$$

Solving for T_{i2}

$$T_{i2} = \left(\frac{T_{i1}}{L} \right) + \left(1 - \frac{1}{L} \right) T_p \quad (2.2-26)$$

In the above four equations, the noise temperature contribution of the components with loss can be written $T_{L1} = (L-1)T_p$ and $T_{L2} = T_{L1} / L = (1-1/L)T_p$.

For a receiving system with an LNA, feed loss and follow-up amplifiers, the noise temperature contributions are

$$T_{e1} = T_{\text{LNA1}} + T_{\text{feed1}} + T_{f1} \quad (2.2-27)$$

and

$$T_{e2} = T_{\text{LNA2}} + T_{f2} \quad (2.2-28)$$

where

T_{LNA1} = LNA noise temperature at the feedhorn aperture, reference location 1, K

$T_{\text{LNA2}} = (L_{\text{feed1}} - 1)T_p$ = LNA noise temperature at the LNA input, reference location 2, K

T_{feed1} = loss noise temperature contribution at the loss input, reference location 1, K

T_{f1} = the follow-up amplifiers noise temperature contribution, reference location 1, K

T_{f2} = the follow-up amplifiers noise temperature contribution at the reference location 2 (LNA input), K

The technique for solving noise temperature translations is to use the above Eqs. (2.2-17 through 2.2-26) in terms of T_i and T_e , obtaining T_i from the input noise sources and T_e from the receiving system noise sources as in Eqs. (2.2-27 and 2.2-28).

2.2.5 Noise Temperature and Loss Contributions

Low loss microwave components at room temperature (~ 290 K) contribute ~ 6.7 K noise temperature for 0.1 dB attenuation. Therefore, it is important to keep losses low to achieve lower noise temperature systems. Accurate measurements (Section 2.6) of the transmission components are essential for

the development of low noise components with minimum loss. System design and component selection are equally important.

2.2.6 Receiver Noise Temperature and Noise Figure

Although the noise figure (sometimes called noise factor) concept is not usually used with low noise systems (Section 2.1), the relationship is provided here for convenience. Noise temperature and noise figure for single response receivers are related by [4 (pp. 54, 55, Table 1 first listed definition)]

$$F = 1 + \left(\frac{T_e}{290} \right) \quad (2.2-29)$$

Solving for T_e

$$T_e = (F - 1) 290 \quad (2.2-30)$$

where

F = receiver noise figure, ratio

T_e = effective receiver input noise temperature, K

Mumford [4 (pp. 54, 55, Table 1)] lists nine separate definitions from the literature for the amplifier noise figure. This clearly shows the importance of noise standards.

2.3 Antennas

2.3.1 Antenna Noise Temperature

Following Eq. (2.2-1), the antenna noise temperature T_a is defined

$$T_a = \frac{N_a}{k} \quad (2.3-1)$$

where

T_a = antenna noise temperature, K

N_a = noise power density delivered by the antenna into a matched termination, W/Hz

k = Boltzmann's constant = 1.38065×10^{-23} , J/K

Antenna noise temperature is given by the integral of the product of the surrounding external physical temperature distribution convolved with the antenna response. As given by Rusch [20 (p.73)], in terms of the antenna external blackbody temperature and antenna gain, both in the direction Ω ,

$$T_a = \int_{4\pi} T(\Omega)G(\Omega)d(\Omega) \quad (2.3-2)$$

where

$T(\Omega)$ = equivalent blackbody temperature of area $d(\Omega)$ in direction Ω , K

$G(\Omega)$ = antenna gain in direction Ω , ratio

In terms of the normalized antenna radiation pattern $P(\Omega)$

$$T_a = \frac{\int_{4\pi} T(\Omega)P(\Omega)d(\Omega)}{\int_{4\pi} P(\Omega)d(\Omega)} \quad (2.3-3)$$

Both downlink DSN antenna gain and noise temperature are defined and referenced at either the LNA input or at the feedhorn input (Section 2.5). The maximum antenna gain relative to an isotropic radiator is given by

$$G_m = \frac{4\pi A_e}{\lambda^2} \quad (2.3-4)$$

where

G_m = maximum antenna gain relative to isotropic radiator, ratio

$G_m(\text{dBi})$ = maximum antenna gain relative to isotropic radiator
 $= 10\log(G_m)$

$A_e = \varepsilon A_p = \pi D_e^2 / 4$ = antenna effective area, m^2

ε = antenna gain efficiency (less than 1), ratio

$A_p = \pi D_p^2 / 4$ = physical area, m^2

λ = wavelength, m

D_p = antenna physical diameter, m

D_e = antenna effective diameter, m

It is difficult to determine the noise temperature contribution of the antenna to the system noise temperature by integration of the convolution of the antenna pattern with the noise source distributions, Eq. (2.3-2). There are multiple noise temperature sources, from various antenna structures, contributing to the total antenna noise temperature variation with antenna elevation angle. The forward and rear antenna spillovers intercept the ground and sky differently as a function of elevation angle. The antenna reflecting surfaces contribute to the

system noise temperature as a function of operating frequency from the ohmic I^2R losses of reflection. The leakage through the surface holes and cracks of the reflecting panels, also contribute to the antenna noise temperature [21–23].

A practical approach used by the DSN for determining the antenna contribution to the system noise temperature is to measure the increased noise temperature between the LNA receiving system on the ground and when it is mounted on the antenna. The noise temperature contribution of the DSN antennas has been measured in this manner for many decades for different frequencies and LNA receiving systems. The atmospheric contributions for the ground and antenna-mounted feedcone configurations are measured separately and accounted for, so the increased noise due to the antenna is determined quite accurately.

2.3.2 DSN Antennas

A performance handbook is available [24] for the Deep Space Network (DSN). The handbook modules provide performance values of the uplink and downlink telecommunications link parameters between spacecraft and the DSN. These modules are updated as new capabilities and data (such as the antenna gain and noise temperature) become available. These modules document the DSN antennas at each of the operating frequencies in more detail than appropriate for this chapter. Current downlink values for the Goldstone, California, station antennas parameters are listed in Table 2-2. The Australian and Spanish antennas have similar values; these include the effect of the higher atmospheric losses.

The front-end loss for a DSN antenna feed assembly is determined by the difference between the system noise temperature at the feedhorn aperture

Table 2-2. DSN Goldstone large ground antennas downlink performance for 25-percent weather and zenith antenna-pointing elevation angle.

Antenna	Freq. Band	Gain (dBi)	Noise Temp. (K)	G/T (dB)	HPBW (deg)
34-m BWG	S	56.8	36.8	41.1	0.23
	X	68.0	33.0	52.9	0.063
	Ka	78.5	31.0	63.6	0.017
34-m HEF	S	56.0	38.0	40.2	0.23
	X	68.1	19.8	55.1	0.063
	Ka	NA	NA	NA	NA
70-m	S	63.4	22.0	50.0	0.11
	X	74.4	20.6	61.3	0.031
	Ka	NA	NA	NA	NA

(system reference location 1), and at the LNA input (system reference location 2). Reference location 1 at the feedhorn aperture is shown in Figs. 2-2 (X-band feedhorn) and 2-8 (feedhorn aperture). Reference location 2 at the LNA input is shown in Fig. 2-12. The DSN calibration procedure for feedcone assembly noise temperature measurements is described in Section 2.5. For precise calibrations of systems with distributed loss between these reference locations it is necessary to translate the various noise temperatures to a common system reference location. This is accomplished with the equations summarized in Table 2-3.

2.3.3 Antenna External Noise Sources

The Cosmic Microwave Background (CMB) and the atmosphere contribute the minimum external incident noise temperature contributions to the DSN antennas. The effects of the ground environment can be reduced by antenna design.

As discussed in Section 2.2.3, the DSN treats the cosmic noise contribution as frequency independent consistent with the Rayleigh-Jeans approximation for the range of frequencies in use. The cosmic microwave foreground (CMF) temperature as discussed in Section 2.1, is small compared to the CMB and is currently not included or considered as a DSN antenna noise contributor.



Fig. 2-8. Goldstone 70-m antenna XTR cone X-band feedhorn aperture reference location 1.

Table 2-3. Noise Temperature Equations Summary.

Items	Equations	Text Eqns.
General:		
(1)	$M = G / T$	2.5-1
(2)	$T_{op} = T_i + T_e$	2.2-4
(3)	$T_{op1} = LT_{op2}$	2.2-20
(4)	$T_{i1} = LT_{i2} - (L-1)T_p$	2.2-25
(5)	$T_{i2} = T_{i1} / L + (1-1/L)T_p$	2.2-26
(6)	$T_{e1} = LT_{e2} + (L-1)T_p$	2.2-23
(7)	$T_{e2} = T_{e1} / L - (1-1/L)T_p$	2.2-24
(8)	$L = (T_p + T_{e1}) / (T_p + T_{e2})$	2.6-10
DSN Application:		
(9)	$T_{op1} = L_{feed}T_{op2}$	2.2-20
(10)	$T_{i1} = L_{feed}T_{i2} - T_{feed1} = T_{sky1} + T_{ant1} + T_{dichroic1}$	2.2-25
(11)	$T_{i2} = T_{i1} / L_{feed} + T_{feed2} = T_{sky2} + T_{ant2} + T_{dichroic2} + T_{feed2}$	2.2-26
(12)	$T_{e1} = L_{feed}T_{e2} + T_{feed1} = T_{LNA1} + T_{feed1} + T_{f1}$	2.5-3
(13)	$T_{e2} = T_{e1} / L_{feed} - T_{feed2} = T_{LNA2} + T_{f2}$	2.5-4
(14)	$T_{feed1} = (L_{feed} - 1)T_p$	2.5-18
(15)	$T_{feed2} = (1 - 1 / L_{feed})T_p$	2.5-9
(16)	$T_{sky1} = L_{feed}T_{sky2}$	*
(17)	$T_{ant1} = L_{feed}T_{ant2}$	*
(18)	$T_{feed1} = L_{feed}T_{feed2}$	2.5-8
(19)	$T_{LNA1} = L_{feed}T_{LNA2}$	2.5-6
(20)	$T_{f1} = L_{feed}T_{f2}$	2.5-7
(21)	$L_{feed} = (T_p + T_{e1}) / (T_p + T_{e2})$	2.5-16
(22)	$T_e = (T_h - Y_{ch}T_c) / (Y_{ch} - 1)$	2.2-7
(23)	$T_f = (T_h + T_e) / Y_{oo} - T_{cryo} / G_{LNA}$	2.6-8
(24)	$T_f = [T_h + T_{LNA} - (Y_{oo}T_{cryo} / G_{LNA})] / (Y_{oo} - 1)$	2.6-9
(25)	$T_{op} = (T_h + T_e) / Y_{ah}$	2.2-8

*Not specifically referenced in text

2.3.3.1 Atmosphere. T_{sky} is the combined measured incident noise temperature of the atmosphere and the CMB as defined at the feedhorn aperture (reference location 1), for each of the multiple receiving systems on each DSN antenna. Sky noise temperature measurements are important for noise temperature calibrations and can be measured with a water vapor radiometer (WVR) as discussed in Chapter 6, a surface weather model [24, module 105] or antenna “tipping” measurements.

The following describes an antenna tipping analysis for T_{sky} . Since the CMB noise is incident on and attenuated by the atmosphere, the sky noise temperature incident on the antenna is expressed by

$$T_{\text{sky}} = T_{\text{atm}} + \frac{T_{\text{CMB}}}{L_{\text{atm}}} \quad (2.3-5)$$

where

T_{sky} = sky noise temperature due to the attenuated CMB and atmosphere, K

T_{atm} = noise temperature contribution of the atmosphere, incident on the antenna, K

L_{atm} = loss due to the atmosphere, ratio

$T_{\text{CMB}} = 2.725$, K

The atmospheric noise temperature contribution due to its loss is given by

$$T_{\text{atm}} = \left(1 - \frac{1}{L_{\text{atm}}}\right) T_{\text{patm}} \quad (2.3-6)$$

where

T_{patm} = physical temperature of an equivalent uniform atmosphere, K

Substituting T_{atm} into Eq. (2.3-5)

$$T_{\text{sky}} = \frac{T_{\text{CMB}}}{L_{\text{atm}}} + \left(1 - \frac{1}{L_{\text{atm}}}\right) T_{\text{patm}} \quad (2.3-7)$$

Accurate system noise temperature calibration measurements require “clear weather.” Clear weather, is defined as having a cumulative distribution (CD) of 0.25 or less; in this chapter a CD of 0.25 is used. The equation, $T_{\text{patm}} = 255 + 25 \text{ CD}$ [24, (105B, p. 10, Eq. (1))], provides an estimate of

261.25 K during clear weather. This value for $T_{p\text{atm}}$ combined with T_{CMB} and measurement of L_{atm} provides an estimate of T_{sky} with Eq. (2.3-7).

The system noise temperature, T_{op} defined at the feedhorn aperture reference location (Fig. 2-8) for a ground antenna and receiving system is given by

$$T_{\text{op}} = T_{\text{sky}} + T_{\text{AMW}} \quad (2.3-8)$$

where

$$T_{\text{AMW}} = T_{\text{ant}} + T_{\text{feed}} + T_{\text{LNA}} + T_f = \text{antenna microwave system noise temperature, K.}$$

Accounting for the difference in the antenna noise temperature change with elevation angle using $\Delta T_{\text{ant}} = \Delta T_{\text{AMW}}$ (Fig. 2-9), the difference in the sky noise temperature, ΔT_{sky} , between elevation angles 1 and 2 is given by

$$\Delta T_{\text{sky}} = \Delta T_{\text{op}} - \Delta T_{\text{ant}} = (T_{p\text{atm}} - T_{\text{CMB}}) \left(\left(\frac{1}{L_{\text{atm1}}} \right) - \left(\frac{1}{L_{\text{atm2}}} \right) \right) \quad (2.3-9)$$

where

$$T_{\text{op1,2}} = \text{system noise temperature at antenna elevation angles 1 or 2, K}$$

$$L_{\text{atm1,2}} = \text{atmosphere loss at elevation angles 1 or 2, ratio}$$

$$T_{\text{ant1,2}} = \text{antenna noise temperature at elevation angles 1 or 2, K}$$

$$\Delta T_{\text{op}} = T_{\text{op2}} - T_{\text{op1}}, \text{ K}$$

$$\Delta T_{\text{ant}} = T_{\text{ant2}} - T_{\text{ant1}}, \text{ K}$$

The propagation attenuation through the atmosphere at elevation angle EL [26 (p. 22)] for a homogeneous atmosphere, in terms of the zenith atmospheric attenuation, A_{atmZ} , using a flat-Earth model, is given (in dB) by

$$A_{\text{atm}} = \frac{A_{\text{atmZ}}}{\sin \text{EL}} \quad (2.3-10)$$

For elevation angles 1 and 2

$$A_{\text{atm1}} = \frac{A_{\text{atmZ}}}{\sin \text{EL}_1} \quad (2.3-11)$$

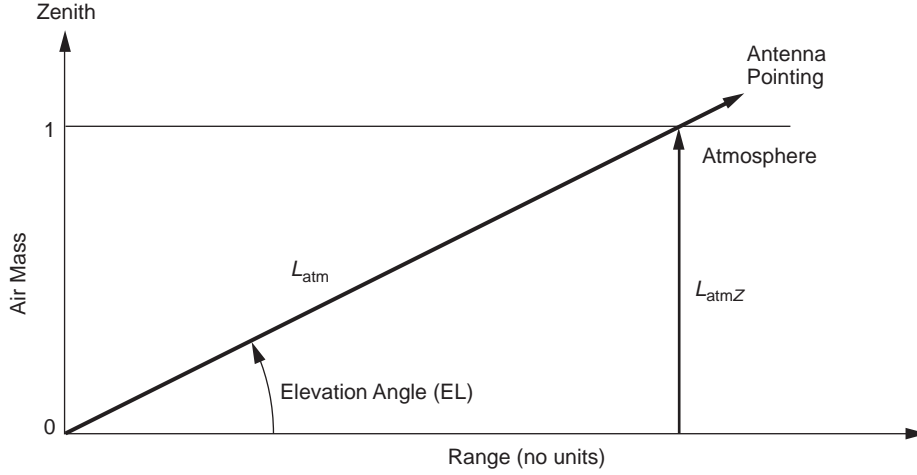


Fig. 2-9. Representation of ground antenna pointing through the atmosphere at elevation pointing angle, EL.

$$A_{\text{atm}2} = \frac{A_{\text{atm}Z}}{\sin \text{EL}_2} \quad (2.3-12)$$

Combining with Eq. (2.3-9) and using $L = 10^{(A/10)}$ results in

$$\Delta T_{\text{sky}} = \Delta T_{\text{op}} - \Delta T_{\text{ant}} = (T_{\text{patm}} - T_{\text{CMB}}) \left(10^{\left(\frac{-A_{\text{atm}Z}}{10 \sin \text{EL}_1} \right)} - 10^{\left(\frac{-A_{\text{atm}Z}}{10 \sin \text{EL}_2} \right)} \right) \quad (2.3-13)$$

A solution can be obtained with elevation angles $\text{EL}_1 = 90$ deg (zenith) using $L_{\text{atm}} = L_{\text{atm}Z}$ for 1 air mass (AM) and $\text{EL}_2 = 30$ deg using $L_{\text{atm}} = (L_{\text{atm}Z})^2$ for 2 air masses

$$\Delta T_{\text{sky}} = \Delta T_{\text{op}} - \Delta T_{\text{ant}} = (T_{\text{patm}} - T_{\text{CMB}}) \left(\left(\frac{1}{L_{\text{atm}Z}} \right) - \left(\frac{1}{L_{\text{atm}Z}} \right)^2 \right) \quad (2.3-14)$$

Solving this quadratic equation for $1/L_{\text{atm}Z}$ and inverting

$$L_{\text{atm}Z} = \frac{2}{1 + \sqrt{1 - 4Q}} \quad (2.3-15)$$

where

$$Q = (\Delta T_{\text{op}} - \Delta T_{\text{ant}}) / (T_{p\text{atm}} - T_{\text{CMB}}), \text{ ratio}$$

$$T_{\text{op1}} = T_{\text{op90}} = T_{\text{op}} \text{ at 90-deg elevation angle, K}$$

$$T_{\text{op2}} = T_{\text{op30}} = T_{\text{op}} \text{ at 30-deg elevation angle, K}$$

$$T_{\text{ant1}} = T_{\text{ant90}} = T_{\text{ant}} \text{ at 90-deg elevation angle, K}$$

$$T_{\text{ant2}} = T_{\text{ant30}} = T_{\text{ant}} \text{ at 30-deg elevation angle, K}$$

ΔT_{ant} needed for Q in Eq. (2.3-15) for the DSS 13 Goldstone research 34-m antenna operating at X-band (8.425 GHz) obtained from a published analysis [43, Table IV], ignoring both the atmosphere and the “bypass” noise contributions removed from this antenna, has a value of 0.89 K. From Eq. (2.3-9), $\Delta T_{\text{ant}} = \Delta T_{\text{op}} - \Delta T_{\text{sky}}$ is used to calibrate ΔT_{ant} . ΔT_{op} was measured with the DSS 13 antenna on 2005-320 to be 2.432 K (17 measurements between 90 and 30 deg elevation angle), and ΔT_{sky} was measured with the WVR to be 2.217 K during this same period. These values result in $\Delta T_{\text{ant}} = 0.215$ K. Although this is in disagreement with the analysis result of 0.89 K, the measurement value of 0.215 K is used in the following.

The quadratic solution, Eq. (2.3-15) is used with these measured ΔT_{op} and ΔT_{ant} data and with $T_{p\text{atm}} = 261.25$ K and $T_{\text{CMB}} = 2.725$ K giving averaged values of $A_{\text{atmZ}} = 0.0377$ dB and $T_{\text{skyZ}} = 4.961$ K. The measurement resolution (scatter) for A_{atmZ} has a standard deviation of 0.0015 dB for the 17 individual measurements. The calibrated value $\Delta T_{\text{ant}} = 0.215$ K could be used with this same antenna and Eq. (2.3-15) to calibrate the atmosphere at X-band on other days as needed independent of the WVR. Further analysis and measurements are needed for agreement between the measurements and the analysis for ΔT_{ant} .

For future improved atmospheric loss calibrations without the WVR, it seems worthwhile to consider a tipping radiometer system using a horn antenna designed for low sidelobes so that the very small value for ΔT_{ant} compared to the atmosphere can be neglected for the atmospheric calibration using the above quadratic solution for 30- and 90-deg elevation angle measurements.

Figure 2-10 shows the DSS-13 R&D Venus research station’s antenna T_{op} and T_{AMW} values as a function of antenna (a) elevation angle and (b) air mass for clear weather conditions for 2005-347. A 0.0387-dB zenith atmospheric loss for this calculation obtained from the WVR at the same operating frequency results in a very small value for ΔT_{ant} . This is indicated by the value for

T_{AMW} , which is nearly independent of elevation angle. T_{AMW} data as a function of antenna elevation angle will be available for all the DSN antennas in future revisions of the DSN 810-005 document [24].

T_{AMW} is an important parameter describing the DSN receiving systems ground performance independent of weather. T_{AMW} is measured for each DSN antenna at each operational frequency and documented in the DSN 810-005 document [24]. T_{AMW} combined with T_{sky} , Eq.(2.3-8), provides the operational system noise temperature as a function of actual or statistical weather data and for any given antenna elevation angle.

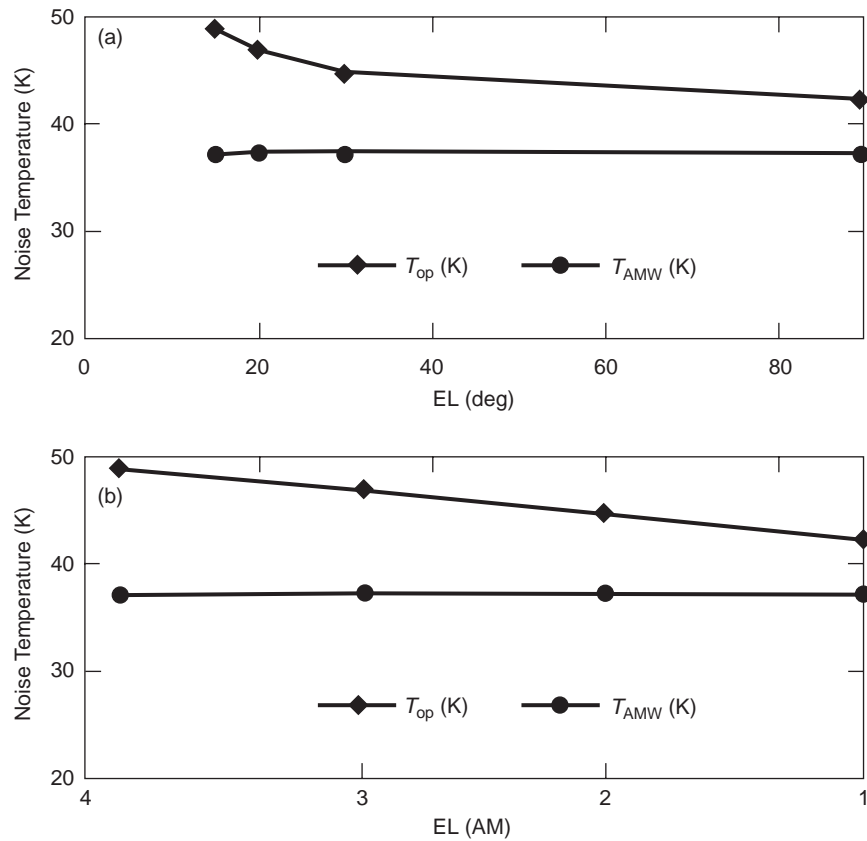


Fig. 2-10. Goldstone DSS 13 34-m BWG antenna X-band system noise temperature T_{op} and T_{AMW} versus antenna elevation angle, 2005-347 doy as functions of (a) elevation angle and (b) air mass.

2.3.3.2 External Noise Sources

Solar noise is the strongest source of observable deep space external noise [24 (module 105 Rev. B, p. 15)]. This noise source should be taken into account when tracking within a few degrees of the Sun. (It is usually considered negligible for DSN antennas at Sun–Earth–Probe (SEP) angles greater than 4 deg.) Figure 2-11 shows the Goldstone High Efficiency (HEF) 34-m antenna X-band system noise temperature increases due to the Sun at various offset angles. This shows the largest increases occurring perpendicular to the antenna quadripod subreflector support structure [5 (module 105 Rev. B, Fig. 12, p. 33)]. An early report shows predicted and measured receiving system noise performance degradations when tracking spacecraft close to the solar limb [27] at S-band (2.297 GHz) with the 64-m Goldstone antenna prior to the upgrade to 70-m diameter. The phase of the 11-year solar cycle is important. The X-band brightness temperature for an active Sun can be two to four times as high as the quiet Sun.

The **Moon** appears as an approximately 240-K blackbody disk with an apparent diameter of about 0.5 deg, similar to the Sun as both seen from Earth. Due to the similar apparent diameters, the solar curves [24 (module 105,

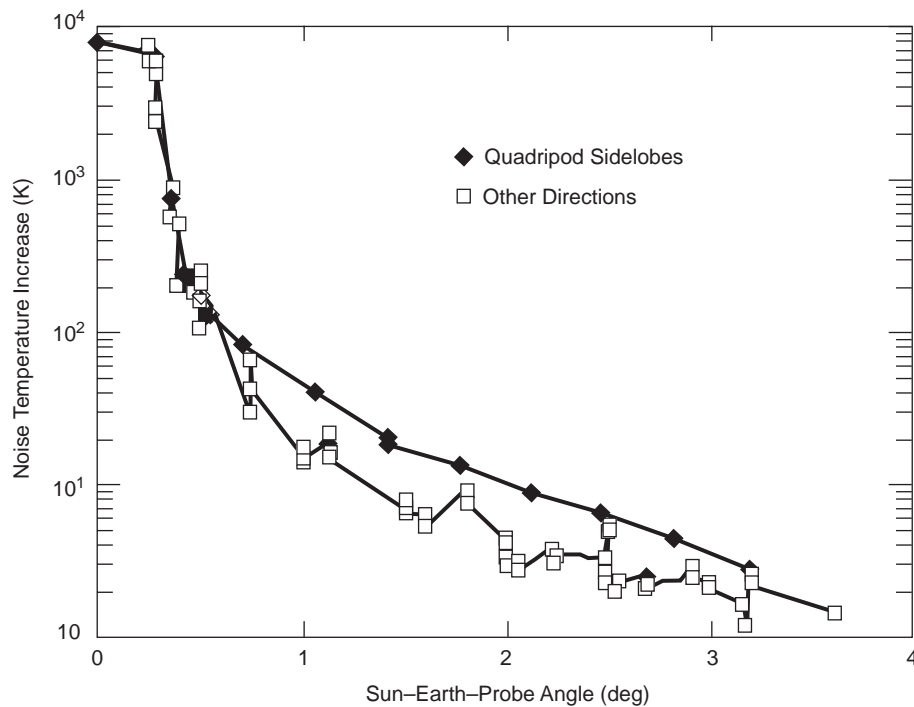


Fig. 2-11. Goldstone High Efficiency (HEF) antenna X-band system noise temperature increases due to the Sun at various offset angles, showing larger increases perpendicular to the antenna quadripod directions.

Rev. B, p. 18)] may be used for lunar calculations, with the noise temperature values scaled by their ‘on point’ values. The clear-sky system noise is included and must be subtracted out before scaling. At antenna pointing offset angles greater than 2 deg, the lunar noise temperature contribution is negligible.

The **Planets** increase the noise temperature within the antenna beam according to the formula [24 (105, Rev. B, p. 19)]

$$T_{\text{pl}} = \left(\frac{T_k G d^2}{16 R^2} \right) e^{-2.77 \left(\frac{\theta}{\theta_o} \right)^2} \quad (2.3-16)$$

where

T_{pl} = increased system noise temperature due to a planet in the antenna beam, K

T_k = blackbody disk temperature of the planet, K

d/R = planet diameter, d , relative to the planet distance, R , ratio

θ/θ_o = angular distance from planet center to antenna beam center, θ , relative to the antenna full half-power beamwidth (HPBW), θ_o , ratio

G = antenna gain, corrected for atmospheric attenuation, ratio

The above calculation of a planet noise temperature contribution to a receiving system noise temperature assumes that the radiating source is small compared to the antenna beamwidth. The constants needed for this calculation are provided in Table 2-4, obtained from the DSN 810-005 document [24 (module 105 Rev. B, Table 20)]. This updates the Venus blackbody disk temperatures at X-and Ka-bands according to the de Pater publication [28]. A graphical approach which is valid for source sizes either less than or greater than the antenna beamwidth developed by Kantak and Slobin [29] as an alternative to Eq. 2.3-17 is also described in module 105, Rev. B [24].

Galactic noise is a frequency-dependent noise contributor from our galaxy (the Milky Way) ranging from a maximum of about 10,000 K at 100 MHz to less than 1 K at 1 GHz [24 (module 105 Rev. B, p. 21)]. This noise source should be taken into account for DSN S-band and X-band frequencies when the antenna beam is pointed toward the Galactic center; it is usually ignored at Ka-band (32 GHz).

Atmospherics and Radio Frequency Interference (RFI) can be disruptive and are not usually predictable. Atmospherics and intermittent RFI cause non-repeatability in system noise temperature measurements. Averaging the results and discarding ‘outlier’ data points can reduce the effect. A stable RFI signal can be detected and characterized within the receiving system

Table 2-4. Planetary parameters and X-band /Ka-band noise temperatures at mean minimum distance from Earth.

	Mercury	Venus	Earth	Mars	Jupiter	Saturn	Uranus	Neptune	Pluto
Equatorial Diameter (km)	4880	12,104	N/A	6794	142,984	120,536	51,118	49,532	2274
Mean Distance from Earth (10 ⁶ km):									
Min.	91.7	41.4	N/A	78.3	628.7	1279.8	2721.4	4354.4	5763.9
Max.	207.5	257.8	N/A	377.5	927.9	1579.0	3020.6	4653.6	6063.1
Mean Distance from Sun:									
(10 ⁶ km)	57.9	108.2	149.6	227.9	778.3	1429.4	2871.0	4504.0	5913.5
AU	0.387	0.723	1.000	1.523	5.203	9.555	19.191	30.107	39.529
Blackbody Disk Temp (K)	625	625 (X-band) 415 (Ka-band)	250–300 ¹	180	152	155	160	160	160
T _{planet} (K) at Mean Minimum Distance:									
X-Band:									
70-m (74.4 dBi gain)	3.05	91.96	N/A	2.33	13.53	2.37	0.10	0.04	0.00
34-m (68.3 dBi gain)	0.75	22.57	N/A	0.57	3.32	0.58	0.02	0.01	0.00
Ka-Band:									
34-m (78.8 dBi gain)	8.39	253.29	N/A	6.43	37.27	6.52	0.27	0.10	0.00

¹ Ocean (250 K) and Land (300 K).

Table taken from 810-005, Module 105, Rev. B, Change 12, May 26, 2006, Table 20 [24].

bandwidth using a spectrum analyzer; the effect may be reduced and or eliminated by changing filters and the operating frequency. This source of interference might not cause erratic measurements but can cause a biased result.

2.4 Low-Noise Amplifiers

2.4.1 Receiver Effective Noise Temperature

The antenna feedhorn, microwave front-end components, low-noise amplifiers (LNAs), and follow-on amplifiers generate internal noise temperature contributions to the front-end-assembly receiving system. These internal contributions are determined and translated according to the equations in Section 2.2 and applied to the receiving system in Section 2.5.

The receiver effective input noise temperature defined at the LNA cryogenic package input is given by (Sections 2.2 and 2.6).

$$T_e = T_{\text{LNA}} + T_f, \quad (2.4-1)$$

where

T_e = receiver effective input noise temperature, K

T_{LNA} = LNA noise temperature, K

T_f = LNA follow-up amplifier noise temperature, K

Maser amplifiers, discussed in Chapter 3, provide the lowest amplifier noise temperatures and have been widely used in the DSN since its inception. HEMT amplifiers, discussed in Chapter 5, are a more recent innovation, and have nearly the low noise performance of masers. They are now also widely used in the DSN. A photograph of the X-band HEMT amplifier used with the Goldstone 70-m antenna XTR feedcone is shown in Fig. 2-12 [30].

2.4.2 Noise Temperature of Cascaded Amplifiers

The effective input noise temperature for a string of cascaded amplifiers is mostly determined by the front-end amplifiers. A receiver consisting of cascaded amplifiers, each with a separate gain and effective input noise temperature has an overall effective input noise temperature given by [4 (p. 22)].

For cascaded amplifiers

$$T_e = T_{e1} + \frac{T_{e2}}{G_1} + \frac{T_{e3}}{G_1 G_2} + \dots + \frac{T_{en}}{G_1 G_2 \dots G_{n-1}} \quad (2.4-2)$$

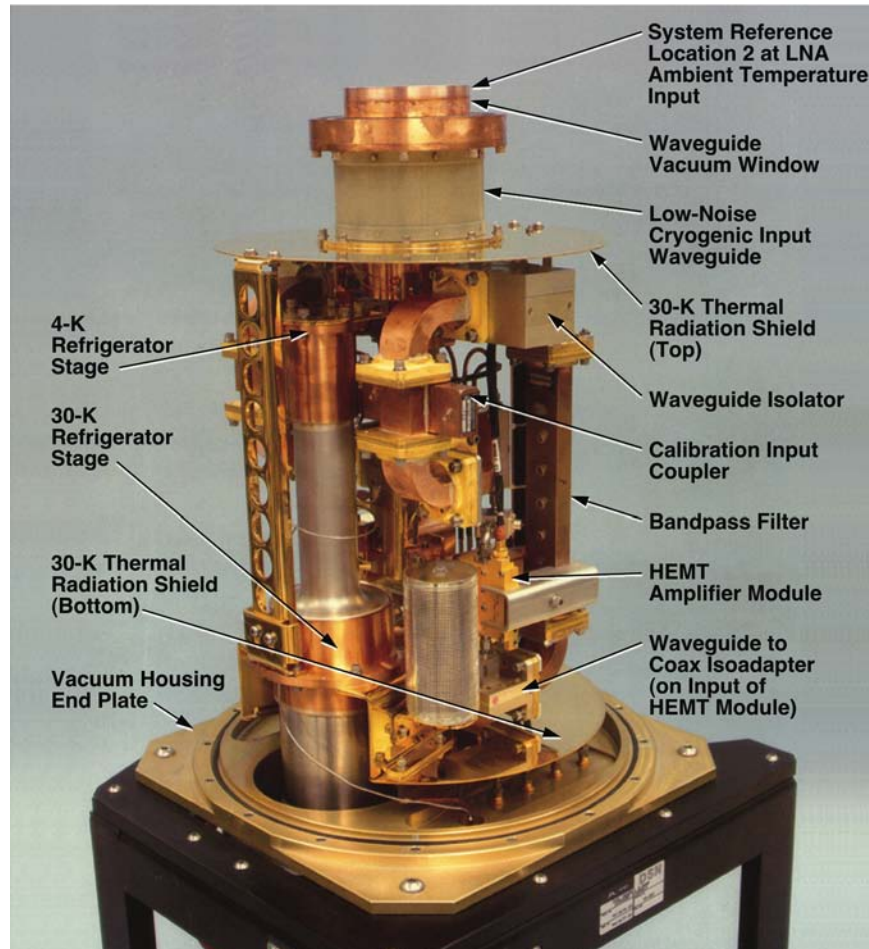


Fig. 2-12. Goldstone 70-m antenna XTR cone X-band HEMT amplifier.

where

T_e = effective input noise temperature of cascaded amplifiers, K

T_{e1} = effective input noise temperature of amplifier 1 at its input, K

T_{e2} = effective input noise temperature of amplifier 2 at its input, K

T_{e3} = effective input noise temperature of amplifier 3 at its input, K

T_{en} = effective input noise temperature of amplifier n at its input, K

G_1 = gain of amplifier 1, ratio

G_2 = gain of amplifier 2, ratio

G_n = gain of amplifier n, ratio

For DSN receiving systems, T_e can be determined with just the first two amplifiers

$$T_e = T_{\text{LNA}} + \frac{T_F}{G_{\text{LNA}}} \quad (2.4-3)$$

where

T_F = effective input noise temperature of LNA “follow-on” or “post” amplifier defined at its input location, K

The receiver noise temperature, T_e , is dominated by the LNA noise temperature, since the DSN LNAs have high gain, relative to the follow-on amplifiers and is generally optimized, minimizing both T_{LNA} and T_f for a well designed system

$$T_f = \frac{T_F}{G_{\text{LNA}}} \ll T_{\text{LNA}} \quad (2.4-4)$$

where

T_f = effective input noise temperature of the post amplifier defined at the LNA input, K

Good performance (low value for T_e) requires both low noise and high gain for the LNA. The “Y-factor” method for measuring T_f is analyzed in Section 2.6 with the results given in Eqs. (2.6-8 and 2.6-9).

2.5 Receiving Systems

2.5.1 Receiving System Figure of Merit

The maximum data rate capability for a communications system [31,32 (p. 2-1)] is proportional to the receiving system antenna gain, which itself is proportional to collecting area, and inversely proportional to the receiving system noise temperature. The receiving system figure of merit, M , is defined as

$$M = \frac{G}{T} \quad (2.5-1)$$

where

M = receiving system figure-of-merit, ratio

$$M, \text{ dB} = 10 \log (M)$$

G = antenna gain relative to isotropic radiator, ratio

$T = T_{\text{op}}$ = system operating noise temperature relative to 1 K, ratio

For a linear receiving system consisting of components with gain and loss, the figure of merit, M , does not change as, a function of the reference location within the receiving system. Moving the reference location within a linear receiving system changes the system gain and noise temperature equally across each component, so that G/T remains constant. Improvement in the receiving system figure of merit requires an increase of the antenna gain (Section 2.3) and/or a reduction in the system noise temperature, T_{op} . Lowering T is in many cases a cost-effective method of increasing G/T . Obtaining either lower system noise temperature or increased antenna area is expensive. System noise-temperature performance is valuable and important for achieving maximum data rates; and therefore, it deserves to be accurately determined and maintained.

2.5.2 Receiving System Operational Noise Temperature

System operating noise temperature is defined as the sum of the external input and internal receiver effective input noise temperatures,

$$T_{\text{op}} = T_i + T_e \quad (2.5-2)$$

where (all terms defined at the same system reference location)

T_{op} = system operating noise temperature, K

T_i = input noise temperature, K

T_e = receiver effective input noise temperature, K

The sum of the input and receiver effective noise temperatures includes contributions from the CMB, atmosphere, ground, antenna, antenna feedhorn, microwave front-end assembly, LNA, and follow-on amplifier. Some of these contributions, such as the LNA, are determined separately from the assembled system. Adding these individual noise temperature contributions requires that each be referenced to the same location.

For DSN bookkeeping it is convenient to use the components T_{CMB} , T_{atm} , T_{ant} , and T_{dichroic} for T_i and T_{LNA} , T_{feed} , and T_f for T_e , at both the feedhorn aperture reference location 1 and the LNA input reference location 2, separated by the feed loss, L_{feed} . For the receiving system noise temperature reference locations

$$T_{e1} = T_{\text{LNA1}} + T_{\text{feed1}} + T_{f1} \quad (2.5-3)$$

and

$$T_{e2} = T_{\text{LNA2}} + T_{f2} \quad (2.5-4)$$

where the noise temperature contribution due to the feed loss at reference location 1 is given by

$$T_{\text{feed1}} = (L_{\text{feed}} - 1)T_p \quad (2.5-5)$$

T_{e2} has no T_{feed} noise temperature contribution since the feed is located “upstream” from the receiver LNA input, reference location 2. The T_{feed} noise contribution becomes part of T_{i2} at the LNA input. With T_{feed} defined separately, the components of T_e are each related by the feed loss, L_{feed}

$$T_{\text{LNA1}} = L_{\text{feed}}T_{\text{LNA2}} \quad (2.5-6)$$

$$T_{f1} = L_{\text{feed}}T_{f2} \quad (2.5-7)$$

and

$$T_{\text{feed1}} = L_{\text{feed}}T_{\text{feed2}} \quad (2.5-8)$$

where the noise temperature contribution due to the feed loss at reference location 2 is given by

$$T_{\text{feed2}} = \left(1 - \frac{1}{L_{\text{feed}}}\right)T_p \quad (2.5-9)$$

When these DSN terms are manipulated and combined for the resultant T_{e1} and T_{e2} values, Eqs. (2.2-23 through 2.2-26) provide the correct translation relationships between the reference 1 and 2 locations. The translation equations are summarized in Table 2-3.

2.5.2.1 Calibration Example. The X-band Transmit and Receive (XTR) feedcone assemblies installed in the DSN 70-m antennas were calibrated beginning in 2000. This section provides a description of the calibration, including details of the noise temperature measurements.

The feeds are installed in the three equipment feedcone assemblies mounted on the dish surface, in a circle, near the center of the dish. From a given feed,

the signal proceeds by waveguide to the front-end equipment located in the designated feedcone assembly. In response to the NASA Cassini mission request for high power X-band uplink, the X-band receive operational (XRO) feedcone assembly containing the X-band maser LNAs was replaced with the X-band transmit receive (XTR) feedcone assembly on the three DSN 70-m antennas. This was accomplished with the addition of a transmit junction to accommodate the X-band uplink capability. A retractable S-/X-band dichroic is installed just above the feedhorn. With the dichroic plate retracted, the system is capable of receiving or transmitting X-band independently or simultaneously. With the dichroic plate extended, the system is capable of

- 1) Receive or transmit S-band independently or simultaneously
- 2) Receive or transmit X-band independently or simultaneously
- 3) Receive S-and X-band simultaneously while transmitting either S-band or X-band

When the XRO feedcone assembly was replaced by the XTR feedcone assembly, an additional loss was incorporated from the transmit junction. Furthermore the maser LNAs in the XRO feedcone assembly were replaced by the high electron mobility transistor (HEMT) LNAs in the XTR feedcone assembly. HEMTs have higher noise temperatures than the maser LNAs. However, the overall receiving system noise temperature with the XTR feedcone assembly was lower than that with the XRO feedcone assembly. This was achieved with development of a diplexed feed [33 (X-band portion)] where the transmit junction is combined with the feedhorn design and by cooling selected waveguide “front-end” components in the low-temperature cryogenic package. A photograph of the X-band HEMT LNA is shown in Fig. 2-12.

A noise temperature comparison of the XRO and XTR feedcone assemblies system noise temperatures mounted on the Goldstone 70-m antenna is shown in Fig. 2-13 for X-band, zenith pointing, and clear weather. The noise temperature values shown have been updated since the original publication [30], consistent with the DSN no longer using Planck’s radiation law noise power reduction at higher frequency as discussed in Section 2.2.3. Therefore, the CMB noise temperature has been changed from an earlier publication value of 2.5 K for X-band to 2.725 K for this updated figure. A sky brightness temperature (combined CMB and atmosphere noise contribution) of 4.8 K is used as compared with the original 4.6 K [30] value. The 0.2 K increase used for the CMB value and a similar decrease of 0.2 K in the receiver system noise temperatures are consistent with the Rayleigh-Jeans approximation. These changes cancel so that the final total system noise temperatures for both feedcones are unchanged.

The noise temperature calibration for DSN front-end assemblies typically uses an ambient calibration load first extended over and then retracted from the

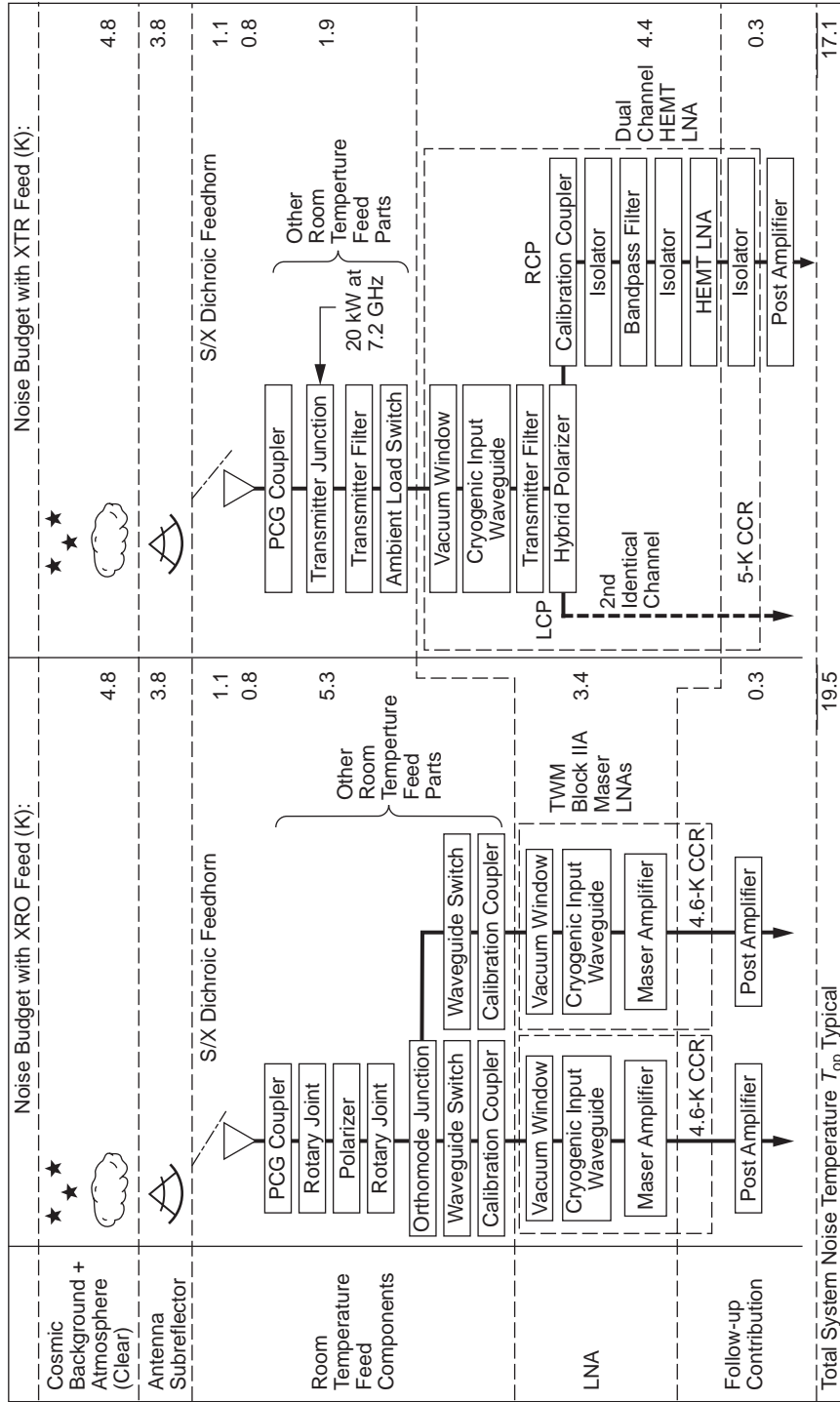


Fig. 2-13. Goldstone 70-m antenna new XTR diplexed feedhorne noise temperature performance defined at feedhorne aperture reference location 1 compared with replaced XRO feedhorne at X-band, zenith and clear weather.

feedhorn aperture input for BWG antennas, or a waveguide switch ambient load for non-BWG antennas as shown in Fig. 2-14 (a) and (b). The sensor for the physical temperature readout is located in the ambient load, in close proximity to the feed assembly. For this reason, the noise temperature calibrations use this same physical temperature, T_p , for both the calibration load and the feed assembly. With the waveguide losses and the ambient calibration load at the same physical temperature, there is no difference for noise measurements between locating the calibration load at the feedhorn aperture, the waveguide switch, or the LNA input. A complete noise temperature calibration sequence for a DSN antenna front-end assembly comprises three separate measurements, a, b, and c. This calibration sequence is required for each newly implemented microwave assembly. Some of these calibrations are also required following maintenance, upgrade, and/or repair. These measurements are performed pointing toward zenith on a clear day, and each requires T_{sky} input (Section 2.6). The three calibration categories are:

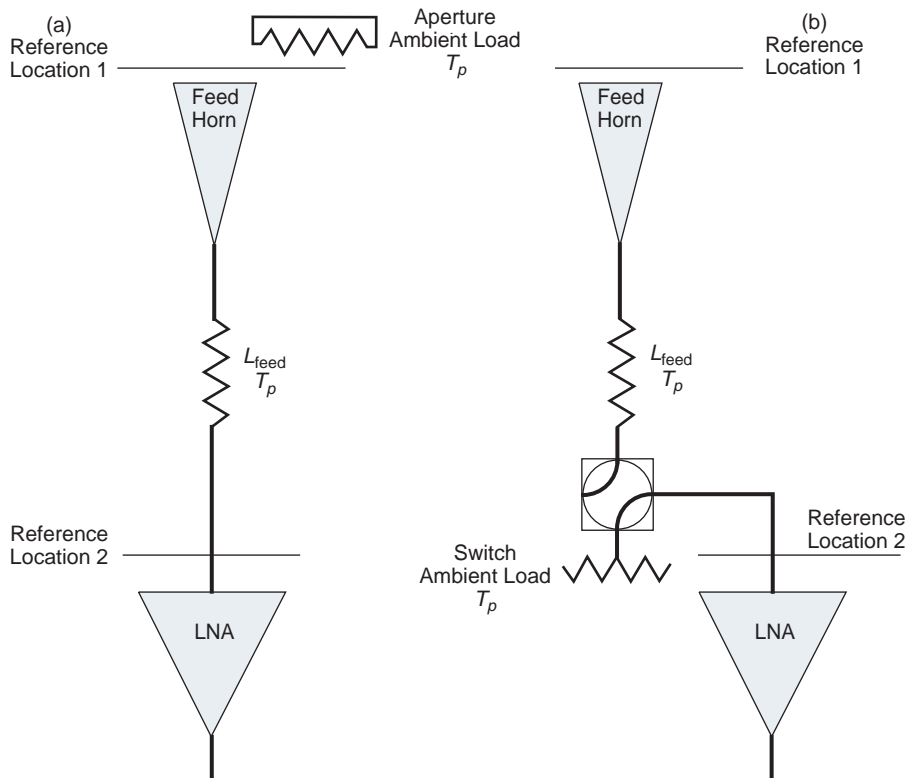


Fig. 2-14. Noise temperature calibration configurations for DSN feed assembly and LNA receiving systems: (a) aperture ambient load BWG antennas and (b) switch ambient load non-BWG antennas.

- 1) **LNA noise temperature (calibration a):** Determine the noise temperature of the LNA, T_{LNA2} defined at the LNA ambient temperature input, system reference location 2, Fig. 2-15.
- 2) **Feed assembly loss (calibration b):** Determine the feed assembly loss, L_{feed} , Fig. 2-16.
- 3) **System noise temperature (calibration c):** With the front-end assembly installed on the antenna, determine the system noise temperature parameter values for T_{op} , T_{AMW} , T_{ant} , and T_{UWV} , all defined at the feedhorn aperture, system reference location 1 shown in Fig. 2-17.

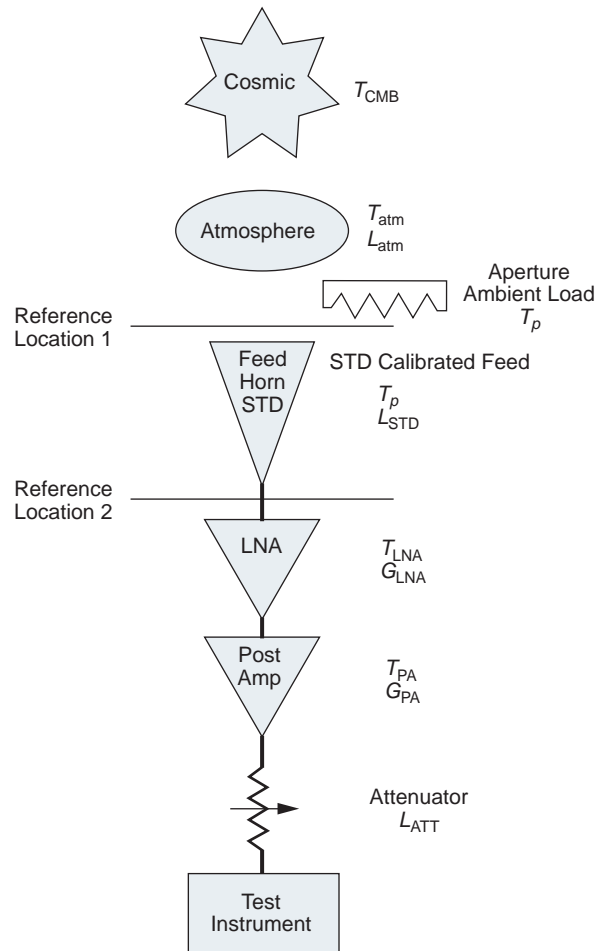


Fig. 2-15. Calibration a: DSN LNA noise temperature calibration configuration.

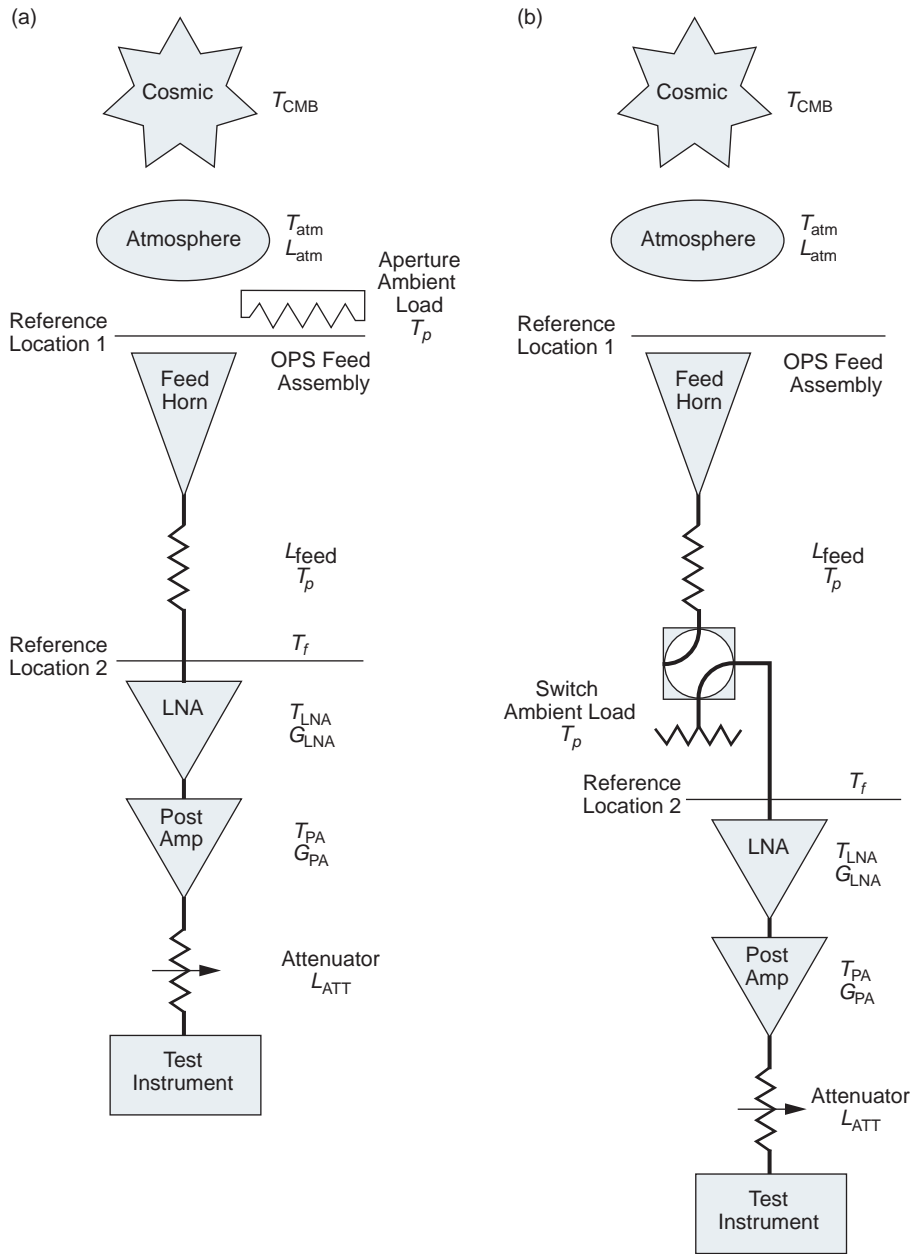


Fig. 2-16. Calibration b: DSN operational feed assembly noise temperature calibration configuration: (a) aperture load and (b) switch ambient load.

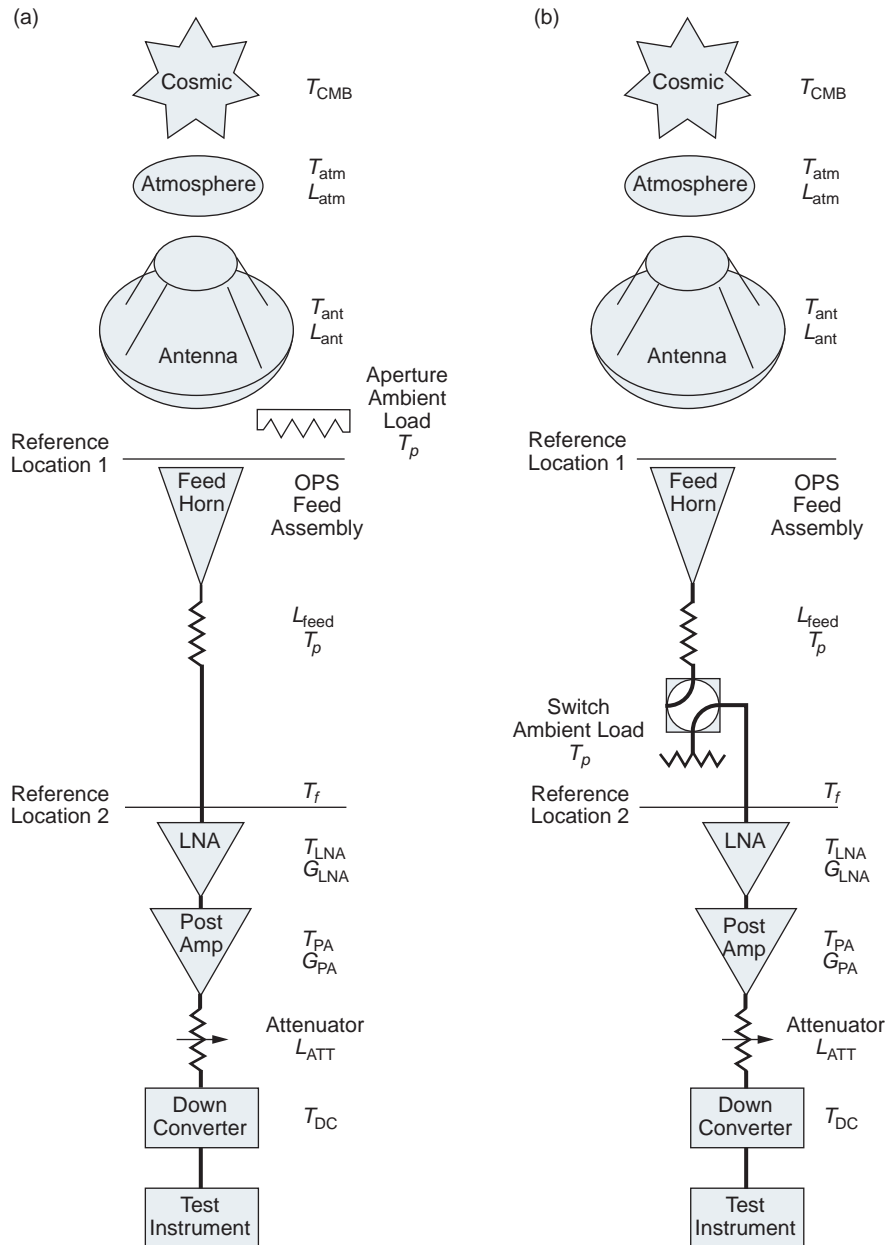


Fig. 2-17. Calibration c: DSN operational feed assembly noise temperature calibration configuration: (a) aperture ambient load and (b) switch ambient load.

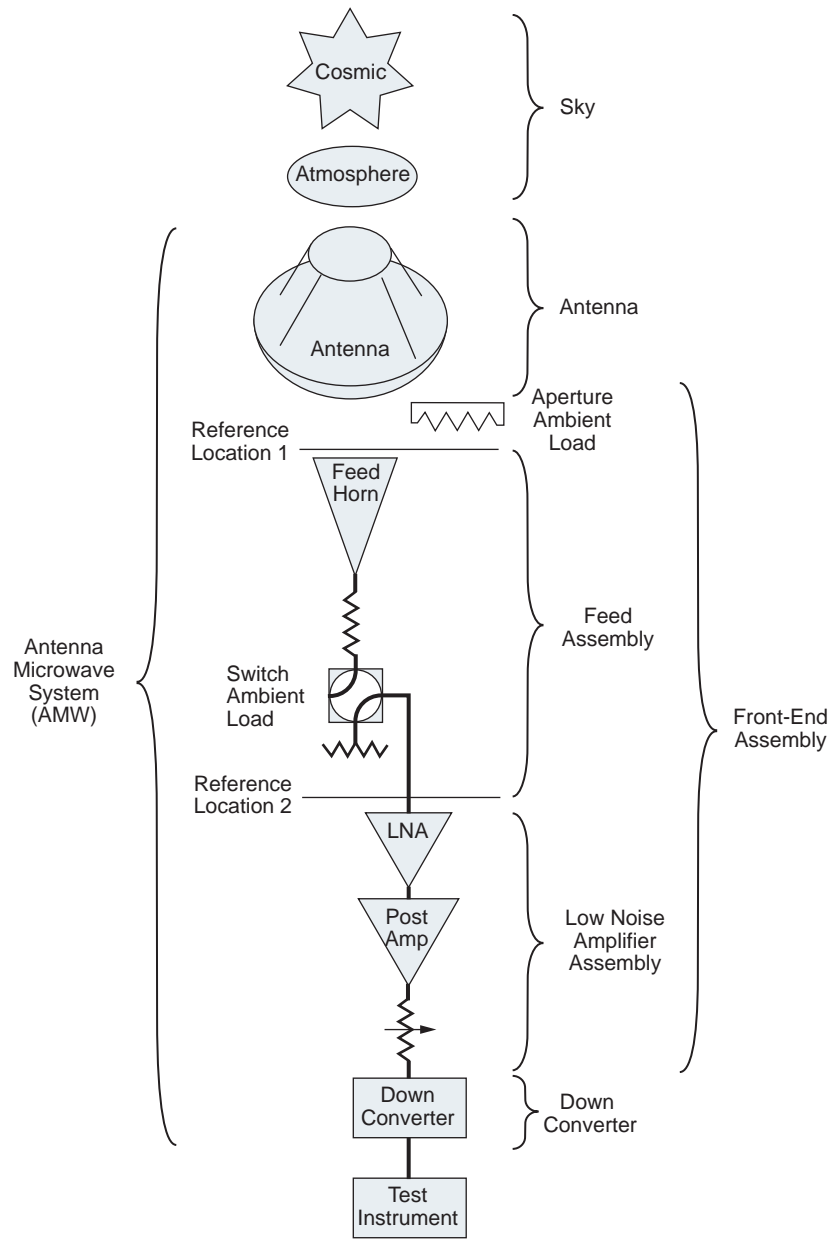


Fig. 2-18. DSN front-end assembly noise temperature calibration configuration components for aperture ambient load or switch ambient load.

2.5.2.2 LNA Noise Temperature (Calibration a). A JPL calibrated standard horn connects directly to the LNA (substituting for the operational feed assembly). The calibrated standard (std) feedhorn viewing the sky pointed to zenith is used as the cold load to measure T_e . The external input noise temperature, T_{i2} , to the LNA is given by

$$T_{i2} = T_{\text{sky}2} + T_{\text{std}2} \quad (2.5-10)$$

Substituting for $T_{\text{sky}2}$

$$T_{i2} = \frac{T_{\text{sky}1}}{L_{\text{std}}} + T_{\text{std}2} = 4.76 + 2.72 = 7.48 \text{ K} \quad (2.5-11)$$

where (values for this example)

T_{i2} = combined sky noise and standard feed loss defined at LNA input reference location 2, K

$T_{\text{sky}2}$ = sky noise temperature defined at the LNA input reference location 2, K

$T_{\text{sky}1} = 4.800$ = sky noise temperature due to the combined atmosphere and CMB, defined at the standard (std) feedhorn aperture reference location 1, K

$T_{\text{std}2} = (1 - 1/L_{\text{std}})T_p = 2.7243$ = noise temperature of the calibrated standard feedhorn loss at the LNA input reference 2, K

$L_{\text{std}} = 1.009253$ (0.040 dB) = loss of the calibrated standard feedhorn between the aperture and the LNA input, ratio

$T_p = 297.1500$ (24.0000 C) = physical temperature of the feedhorn loss, K

Using T_{i2} from Eq. (2.5-11) with the Y-factor equation, Item 22 of Table 2-3, for T_{e2} (LNA and follow-on amplifier) noise temperature, gives

$$T_{e2} = \frac{T_p - Y_{ah}T_{i2}}{Y_{ah} - 1} = 4.70 \text{ K} \quad (2.5-12)$$

where (values for this example)

T_{e2} = receiving system effective noise temperature at LNA input reference location 2, K

$Y_{ah} = 24.7742$ (13.9400 dB) = hot (ambient) load and antenna Y -factor, ratio

$T_p = 297.1500$ (24.0000 C) = physical temperature of the hot (ambient) load, K

The follow-on noise temperature contribution (T_f) given by Eq. (2.6-8), with terms defined there and ignoring the smaller second term for this application with $Y_{oo} = 977.23722$ (29.9000 dB) is given by

$$T_{f2} = \frac{T_p + T_{e2}}{Y_{oo}} = 0.309 \text{ K} \quad (2.5-13)$$

and with Eq. (2.5-12) gives

$$T_{\text{LNA}2} = T_{e2} - T_{f2} = 4.704 - 0.309 = 4.395 \text{ K} \quad (2.5-14)$$

Although the DSN calibrates their LNA noise temperatures with an unobstructed view of the sky using a calibrated standard horn pointed toward zenith in place of a cold load, this calibration could be accomplished in the laboratory using two calibrated loads, a hot (ambient) load and a calibrated cooled load. The application of a standard horn as the cold load for calibrating LNAs has been used in the DSN for a number of years.

2.5.2.3 Feed Assembly Loss (Calibration b). The operational feed assembly is ready for evaluation after calibration and installation of the LNA in the front-end assembly. The receiver noise temperature is calibrated at the feedhorn aperture reference location 1, similar to calibration a, with Eq. (2.5-12). For the XTR feedcone pointed toward zenith

$$T_{e1} = \frac{T_p - Y_{ah}T_{i1}}{Y_{ah} - 1} = 7.497 \text{ K} \quad (2.5-15)$$

where (values for this example)

T_{e1} = receiving system effective input noise temperature defined at the feedhorn aperture reference location 1, K

$T_p = 297.1500$ (24.0000 C) = physical temperature of the ambient load, K

$T_{i1} = T_{\text{sky}1} = 4.8000$ = input noise temperature due to the combined atmosphere and CMB, defined at the feedhorn aperture reference location 1, K

$Y_{ah} = P_h / P_a = 24.7738$ (13.93992 dB) = hot (ambient) load and antenna Y -factor, ratio

The XTR front-end feed assembly loss can be calculated using Eq. (2.6-10) with the T_{e1} value from Eq. (2.5-15) = 7.497

$$L_{\text{feed}} = \frac{T_p + T_{e1}}{T_p + T_{e2}} = 1.0092296 \text{ ratio} (= 0.03990 \text{ dB}) \quad (2.5-16)$$

This uses $T_{\text{LNA2}} + T_{f2}$ for T_{e2} and the first two numerator terms of Item 24 in Table 2-3 for T_{f2}

$$T_{f2} = \frac{T_p + T_{\text{LNA2}}}{Y_{oo} - 1} = 0.31609 \text{ K} \quad (2.5-17)$$

where (for Eqs. 2.5-16 and 2.5-17)

L_{feed} = feed assembly loss, ratio

$T_{e2} = T_{\text{LNA2}} + T_{f2} = 4.395$ (from Eq. (2.5-14)) + 0.31609 (from Eq. (2.5-17)) = 4.711 = receiving system effective input noise temperature defined at the LNA input reference location 2, K

T_{f2} = follow-up amplifier noise temperature contribution defined at the LNA input reference location 2, K

$T_p = 297.1500$ (24.0000 C) = physical and noise temperature of the ambient load, K

$Y_{oo} = 954.99259$ (29.8000 dB) = LNA on and off Y -factor, ratio

The noise temperature contribution of the feed assembly loss, defined at the feedhorn aperture is

$$T_{\text{feed1}} = (L_{\text{feed}} - 1)T_p = (1.0092296 - 1) 297.1500 = 2.743 \text{ K} \quad (2.5-18)$$

This completes the front-end assembly evaluation at the ground site, prior to installation on the antenna.

2.5.2.4 System Noise Temperature (Calibration c). With the installation of the front-end assembly on the antenna, the system noise temperature, T_{op} , and the noise contributions from the major components of the system are determined using items 9 and 25 of Table 2-3.

$$T_{op1} = L_{feed} \left(\frac{T_p + T_{e2}}{Y_{ah}} \right) = 17.12 \text{ K} \quad (2.5-19)$$

where

$T_{op1} = T_{op}$ = system noise temperature, front-end assembly on antenna, defined at the feedhorn aperture reference location 1, K

$L_{feed} = 1.0092296$ (0.03990 dB) = feed assembly loss, ratio

$T_p = 297.1500$ (24.00 C) = feed and load physical temperature, K

$T_{e2} = T_{LNA2} + T_{f2} = 4.3950 + 0.2690 = 4.6640$ = receiving system effective input noise temperature at LNA input, reference location 2, K. Note that T_f for calibrations a, b, and c are not identical due to different configurations

$Y_{ah} = P_h / P_a = 17.79099$ (12.50200 dB) = hot (ambient) load and antenna Y -factor ratio

The primary requirements to be verified for a system in the field is the noise contribution of the Antenna Microwave system, T_{AMW} ($T_{AMW} = T_{ant} + T_{UWV}$), microwave front end feed assemble (feed and LNA), T_{UWV} ($= T_{e1}$), and the antenna, T_{ant} all defined at the feedhorn aperture reference location 1. Figure 2-8 shows the feedhorn aperture input of the XTR front end assemble as installed on the Goldstone 70-m antenna. The following analysis determines all these parameters.

The microwave noise contribution, T_{UWV} , using items 12 and 14 of Table 2-3 and the values given above can be determined by

$$\begin{aligned} T_{UWV} = T_{e1} = L_{feed} T_{e2} + (L_{feed} - 1) T_p &= (1.0092296)(4.66399) \\ &+ (0.0092296)(297.1500) = 7.45 \text{ K} \end{aligned} \quad (2.5-20)$$

where

$T_{UWV} = T_{e1}$ = microwave receiver effective input noise temperature defined at the feedhorn aperture reference location 1, K

It is important to determine an equivalent system noise temperature T_{AMW} not accounting for the external contributions of T_{sky} for use in the DSN 810-005 mission interface document [24] as required for the operational missions. T_{AMW} is determined for the XTR feedcone using the values given above

$$T_{AMW} = T_{op1} - T_{sky1} = 17.12 - 4.80 = 12.32 \text{ K} \quad (2.5-21)$$

where

T_{AMW} = antenna-microwave receiver input noise temperature defined at the feed aperture location 1, K

The zenith antenna noise temperature contribution defined at the feedhorn aperture, system reference location 1, is given by

$$T_{ant1} = T_{AMW} - T_{e1} - T_{dichroic1} = 12.32 - 7.45 - 1.10 = 3.77 \text{ K} \quad (2.5-22)$$

For the Goldstone 70-m antenna pointed at zenith, the system noise temperature is defined at the XTR feedhorn aperture input system reference 1 as $T_{op1} = 17.12 \text{ K}$. These results are for a Goldstone “clear weather” day whereas the DSN 810-005 document [24] provides averaged weather performance. Weather statistics are useful for mission planning. The atmospheric contribution of noise temperature and loss as a function of elevation angle and cumulative distribution (CD) value are added to the vacuum zenith noise temperature for the overall system performance needed for operational applications.

It is useful to perform a noise temperature calibration sequence of five or six sequential independent measurements with the antenna pointed toward zenith. This provides statistical results for the system operational noise temperature as well as an analysis of the receiving system nonlinearity (as described in Section 2.6) and the calibration noise diodes.

The calibration noise diodes (not shown in Fig. 2-13) are installed in a separate “noise box” module and connected to the side arm of the “CAL COUPLER,” usually a waveguide directional coupler. With a 35-dB coupler, injecting 100-K noise requires a noise diode capable of generating more than $100 \text{ K} \times 3162.3 = 316,230 \text{ K}$, accounting for cabling and other losses. With the noise diode turned off and a physical temperature of 300 K, the noise temperature coupled into the system is the physical temperature reduced by the 35 dB, or $300/3162.3 = 0.09 \text{ K}$. Low-noise receiving systems require large coupling factors to reduce the noise temperature contribution. It is not necessary to account for this coupling factor beyond using a, b, and c calibrations as long as the coupler termination is at the same physical temperature as the feed. Ignoring resistive losses, the equivalent coupler “main line” loss L , due to the coupler side arm coupling factor L_c is given by $L_c / (L_c - 1)$. For a 35-dB coupler, with $L_c = 3162.3$, $L = 1.000316$ or 0.00137 dB. A resistive attenuator with the same 0.00137 dB loss at 300 K would also contribute 0.09 K.

2.5.2.5 Operational System Noise Temperature Calibrations. The above series of measurements for calibrations a, b, and c serve the engineering purpose of determining the various noise temperature parameters of a new or modified antenna or front-end assembly. In addition, some of these calibrations are repeated routinely to monitor the system performance or to requalify a modified system after system changes have been made. The most likely recalibration would be for the LNA replacement on the antenna or the recalibration of a repaired LNA on the ground to verify the input noise temperature, T_{LNA2} , requiring the use of the gain standard feedhorn and the associated ground instrumentation. In addition to these tests it is necessary to perform system linearity performance verification of the system and confirm that the measurement instrumentation is accurate.

The primary product of the above calibrations is T_{AMW} for calculating the system operating noise temperature with application to tracking spacecraft under varying weather conditions.

$$T_{op} = T_{sky} + T_{AMW} \quad (2.5-23)$$

where

$$T_{sky} = T_{atm} + \frac{T_{CMB}}{L_{atm}} \quad (2.5-24)$$

and

$$T_{AMW} = T_{ant} + T_{feed} + T_{LNA} + T_f \quad (2.5-25)$$

For application to mission operations, these terms are all defined at the feedhorn aperture. Missions can estimate T_{op} for DSN antenna systems using documented values of T_{AMW} [24 (module 101B, Eq. A2, p. 36 and Table A-3, p. 40)] and either measured T_{sky} or statistical data [24 (module 105 B, Eq. 1, p. 10 and Table 13, p. 53)].

For routine system noise temperature calibrations of T_{op} , it is customary to use the Y-factor method switching between the system ambient (hot) load and the antenna, using the known value of $T_{UWV}(T_e)$ with Eq. (2.2-8) (item 25 in Table 2-3). T_{AMW} can also be determined from Eq. (2.5-23) ($T_{AMW} = T_{op} - T_{sky}$), but the T_{op} measurement requires knowing T_e , which could change over time. Routine verification of T_{AMW} can be measured

directly, independent of knowing T_e using $T_c = T_{\text{sky}} + T_{\text{ant}}$, and $T_h = T_p$ with $T_e = (T_h - Y_{ch}T_c / Y_{ch} - 1)$, Eq. (2.2-7) (item 22 in Table 2-3) giving

$$T_{\text{AMW}} = \left(\frac{(T_p - T_{\text{ant}}) - Y_{ah}T_{\text{sky}}}{Y_{ah} - 1} \right) \quad (2.5-26)$$

where

Y_{ah} = Y-factor switching between the antenna (sky) and hot (ambient) load, ratio

T_{sky} data is available in the DSN from a water vapor radiometer. T_{ant} data is available from the initial calibrations on the antenna as shown in Eq. (2.5-22). T_{AMW} combined with T_{sky} as given by the weather statistics for each location determines the overall system noise temperature for each antenna. The T_{AMW} measurement also provides an updated value for $T_{\text{UWV}}(T_e)$ using $T_e = T_{\text{AMW}} - T_{\text{ant}}$.

2.5.2.6 Sources of Noise Temperature Calibration Errors. Table 2-5 shows a, b, and c calibration “1-sigma errors” (Cal a, b, and c in the table). Except for the statistical measurement error, the estimated peak error or ‘limit of error’ for the “systematic errors” are each divided by three for an estimate of an equivalent 1-sigma’ error. This approach [34 (p. 35)] is commonly used for combining the effect of disparate errors for an overall total estimate. Each error is calculated by perturbing the input data, one parameter at a time by the estimated 1σ accuracy, for each type of calibration. The system nonlinearity (NL), voltage standing wave ratio (VSWR), and measurement errors are small compared to the error in T_{sky} ; therefore, they are not included for the a and b calibrations. For calibration c, on the antenna, the DSN receiving system requirement for NL, 0.5-percent peak (0.167 percent 1 sigma) is used. For the 17.1-K T_{op} system noise temperature of the XTR feedcone, the resultant NL error is 0.03 K. The dominant error due to mismatch (VSWR) of the microwave components is given by [13 (p. 14, case 2, error 1)]

$$E_{\text{VSWR}} = \left[\frac{1 - 4S_e S_p}{(S_e S_p + 1)^2} \right] \frac{T_p}{Y_{ah}} \quad (2.5-27)$$

Table 2-5. Parameter errors evaluated for calibrations a, b, and c at the DSN Goldstone DSS 14, 70-m antenna XTR feedcone microwave X-band receive (8.42 GHz).

Parameters Evaluated	Input Parameter 1-sigma Errors (boxed) and Output Parameter 1-sigma Errors (not boxed)							RSS Errors
	$T_{p,C}$	P_{load} , dBm	P_{sky} , dBm	P_{off} , dBm	T_{sky1} , K	A_{STD} , dB		
Cal a	0.10	0.01	0.01	0.33	0.20	0.003		
T_{LNA2} , K = 4.3950	0.0031	0.0285	0.0292	0.0244	0.2063	0.2082	0.297	
T_{LNA} , %	0.072	0.649	0.664	0.555	4.694	4.738	6.76	
Cal b	$T_{p,C}$	P_{load} , dBm	P_{sky} , dBm	P_{off} , dBm	T_{sky1} , K	T_{LNA2} , K		
	0.10	0.01	0.01	0.33	0.20	0.297		
A_{feed} , dB = 0.0399	0.00005	0.00041	0.00042	0.00036	0.00297	0.00427	0.0053	
A_{feed} , %	0.113	1.029	1.055	0.901	7.449	10.714	13.16	
Cal c	$T_{p,C}$	P_{load} , dBm	P_{sky} , dBm	P_{off} , dBm	T_{sky1} , K	T_{LNA2} , K	A_{feed} , dB	
	0.10	0.01	0.01	0.33	0.20	0.297	0.0053	
							NL, K	
							VSWR, K	
							Measurement, K	
							0.1058	
							0.0856	
$T_{UWV}(T_{el})$, K = 7.4496	0.0010	0.0006	0.0000	0.0215	0.0000	0.3000	0.3720	
$T_{UWV}(T_{el})$, %	0.014	0.008	0.000	0.288	0.000	4.027	4.993	
T_{anti} , K = 3.7714	0.0047	0.0388	0.0395	0.0202	0.2000	0.2831	0.3510	
T_{anti} , %	0.124	1.028	1.047	0.537	5.303	7.507	9.308	
T_{f1} , K = 0.2715	0.0001	0.0006	0.0000	0.0215	0.0000	0.0003	0.0003	
T_{f1} , %	0.033	0.231	0.000	7.902	0.000	0.098	0.121	
							0.098	
							0.121	
T_{opt1} , K = 17.1210	0.0057	0.0394	0.0395	0.0012	0.0000	0.0169	0.0209	
T_{opt1} , %	0.033	0.230	0.231	0.007	0.000	0.098	0.122	
T_{AMW1} , K = 12.3210	0.0057	0.0394	0.0395	0.0012	0.2000	0.0169	0.0209	
T_{AMW1} , %	0.046	0.320	0.320	0.010	1.623	0.137	0.170	
							0.232	
							0.859	
							0.695	
							0.152	
							0.0856	
							0.1058	
							0.167	
							0.500	
							0.0856	
							0.1058	
							0.251	
							2.04	

NL = nonlinearity, RSS = root-sum-squared, VSWR = voltage standing wave ratio
 NL error = 0.5% T_{op} divided by 3, VSWR error Eq. (2.5-27) divided by 3 with $S_p = 1.1$ and $S_e = 1.2$

where

E_{VSWR} = error in T_{op} due to mismatched microwave components, K

S_e = LNA input VSWR, ratio

S_p = calibration load input VSWR, ratio

T_p = calibration load physical temperature, K

$Y_{ah} = P_h / P_a$ = hot (ambient) load and antenna Y -factor, ratio

Only the VSWR mismatch between the calibration load and the receiver LNA is needed for calculating the error in T_{op} due to mismatch [13]. Although mismatch in the antenna/LNA receiving system microwave components modifies T_{op} , this is not a measurement error. The VSWR's S_p and S_e for the XTR system at band center of 8.4 GHz are estimated as 1.10 (return loss = -26.4 dB) and 1.20 (return loss = 20.8 dB) for the calibration load and the LNA. With T_p and Y_{ah} values of 297.15 K and 17.79 dB for the calibration load and system, the peak mismatch error is 0.317 K (other mismatch effects are less than 0.003 K and are neglected for this calculation) with 0.1058 K 1-sigma value.

The root sum square (RSS) [34 (p. 35)] of these individual error sources are calculated for each output parameter. The RSS error for the key deliverables is less than 1 percent for T_{opl} and 2 percent for T_{AMW} for the Goldstone XTR feedcone example. The biggest error sources for T_{op} and T_{AMW} are due to the VSWR mismatch and inaccuracy in the T_{sky} calibrations, respectively.

2.6 Measurements

2.6.1 Y-Factor Noise Temperature Calibrations

A widely used technique for the measurement of the system, receiver, and follow-up amplifier noise temperatures is the Y -factor method [4 (p. 26)]. Since thermal noise limits a receiving system's sensitivity performance, it is important to measure this noise source for communication systems. The equations for noise temperature calibrations by the Y -factor method follow.

2.6.1.1 Receiver. The Y -factor power ratio for the receiver effective input noise temperature measurement configuration shown in Fig. 2-19 by switching between the cold and hot loads, as measured at the receiver output, is given by

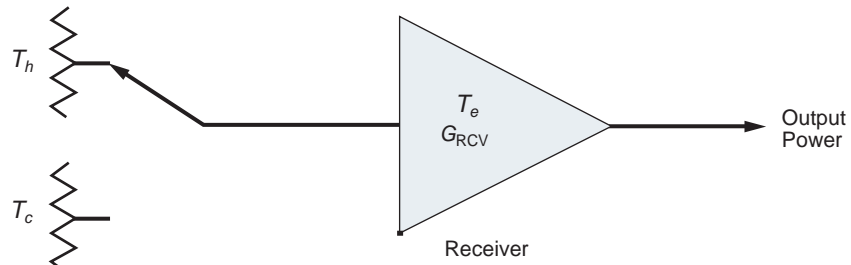


Fig. 2-19. Configuration for determining the receiver noise temperature, T_e , measuring the Y -factor, switching between hot and cold terminations.

$$Y_{ch} = \frac{T_h + T_e}{T_c + T_e} \quad (2.6-1)$$

where

$Y_{ch} = P_h / P_c =$ hot (ambient) and cold load Y -factor, ratio

$T_h =$ physical temperature of the hot (ambient) load, K

$T_c =$ physical temperature of cold load, K

$T_e =$ receiver effective input noise temperature, K

Although the Y -factor ratios are power measurements, both Boltzmann's constant k , and the noise bandwidths cancel, resulting in noise temperature ratios, as shown in Eq. (2.6-1), eliminating the need for their determination. In practice, the system bandwidth is usually restricted with a bandpass filter prior to the power-meter input. This reduces measurement errors due to RFI and variations in bandwidth during the measurement process.

Solving Eq. (2.6-1) for the receiver effective input noise temperature, T_e [5 (p. 11-1)]

$$T_e = \frac{T_h - Y_{ch}T_c}{Y_{ch} - 1} \quad (2.6-2)$$

2.6.1.2 System. With T_e known, a similar Y -factor ratio measurement technique switching the amplifier input between the antenna and the hot load, as shown in the system configuration Fig. 2-20 [37 (p. 41)], results in the Y -factor

$$Y_{ah} = \frac{T_h + T_e}{T_i + T_e} \quad (2.6-3)$$

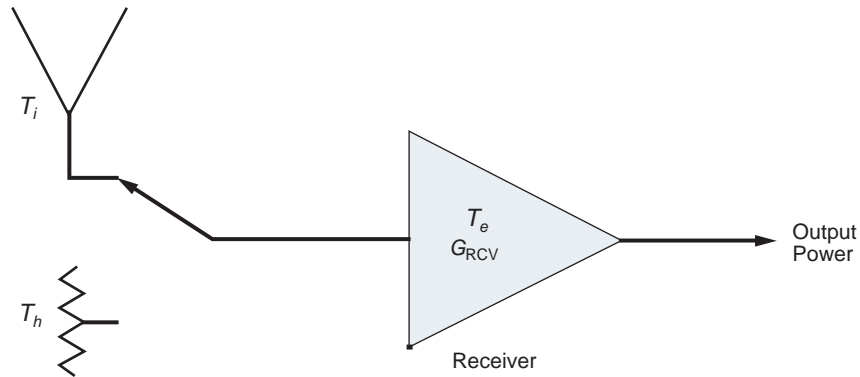


Fig. 2-20. Configuration for determining the system operating noise temperature, T_{op} , measuring the Y -factor, switching between the hot termination and the antenna.

where

T_i = antenna noise temperature, including all external noise inputs such as cosmic, atmosphere, ground radiation and microwave loss effects, K

Using $(T_i + T_e) = T_{\text{op}}$ and solving for T_{op} considering T_e (as known from previous measurement),

$$T_{\text{op}} = \frac{T_h + T_e}{Y_{ah}} \quad (2.6-4)$$

where

$Y_{ah} = P_h / P_a$ = hot (ambient) load and antenna Y -factor, ratio

Manual switching using an external aperture load for measuring system noise temperature is shown in Fig. 2-21. The aperture load is alternately placed over and removed from the horn aperture. Good results have been obtained using commercial resistive material designed for absorbing microwave energy.

2.6.1.3 Antenna. From the above two Y -factor measurements and using $T_{\text{op}} = T_i + T_e$ = system operating noise temperature

$$T_i = T_{\text{op}} - T_e \quad (2.6-5)$$

2.6.1.4 Follow-up amplifiers. The receiving system discussed above consists of an LNA and follow-up amplifiers. T_e is composed of the sum of T_{LNA} and T_f



Fig. 2-21. X-band (8.5-GHz) calibrated feed and LNA system demonstrating a manual aperture load noise temperature measurement technique.

$$T_e = T_{\text{LNA}} + T_f \quad (2.6-6)$$

where

T_{LNA} = LNA effective input noise temperature, K

T_f = follow-up amplifiers noise temperature, K

A convenient method to measure T_f is to perform a Y -factor measurement, turning the LNA on and off. When the LNA is turned off, the post amplifier

input is terminated in the cold load at the LNA cryogenic temperature, T_{cryo} . See Fig. 2-22.

$$Y_{oo} = \frac{(T_h + T_e)G_{\text{LNA}}}{T_{\text{cryo}} + G_{\text{LNA}}T_f} \quad (2.6-7)$$

where

$Y_{oo} = P_{\text{LNA on}} / P_{\text{LNA off}} =$ LNA on and off Y-factor, ratio

$T_{\text{cryo}} =$ physical temperature of LNA (estimated input termination temperature for the follow-up amplifier when LNA turned off), K

$G_{\text{LNA}} =$ LNA gain, ratio

$T_e =$ receiver effective input noise temperature defined at the LNA input, K

$T_h =$ physical hot load temperature (usually ambient load), K

$T_f =$ follow-up amplifiers noise temperature contribution, K

$G_{\text{LNA}}T_f =$ LNA follow-up amplifier noise temperature contribution defined at LNA output, K

Solving Eq. (2.6-7) for T_f

$$T_f = \frac{T_h + T_e}{Y_{oo}} - \frac{T_{\text{cryo}}}{G_{\text{LNA}}} \quad (2.6-8)$$

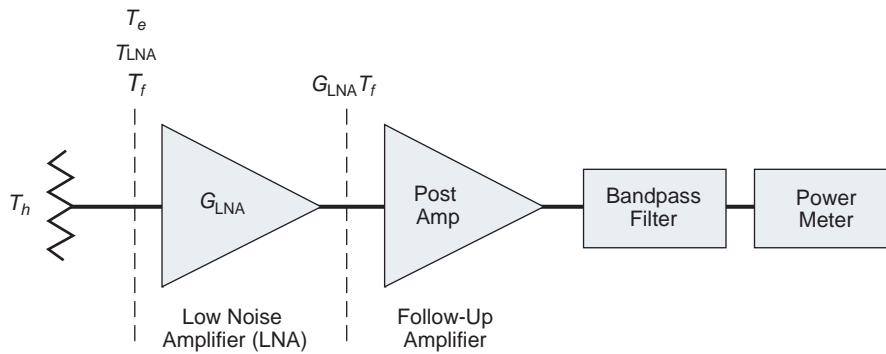


Fig. 2-22. Configuration for determining the follow-up amplifiers noise temperature contribution, T_f , measuring the Y-factor, switching the LNA on and off.

This can also be written using $T_e = T_{\text{LNA}} + T_f$, so that, alternately

$$T_f = \frac{T_h + T_{\text{LNA}} - \frac{Y_{oo} T_{\text{cryo}}}{G_{\text{LNA}}}}{Y_{oo} - 1} \quad (2.6-9)$$

Eq. (2.6-8) is useful when T_e is known and Eq. (2.6-9) is useful when T_{LNA} is known.

2.6.2 Attenuation

As discussed in Section 2.2.5 even small attenuation values in microwave components contribute significant thermal noise in low-noise receiving systems. For low-noise receiving systems, 0.01 dB of attenuation at the receiver input increases the system temperature about 0.67 K (~0.67 K per 0.01 dB). This can reduce the system sensitivity (G/T , dB) by much more than the 0.01 dB loss.

It is important to measure the losses of microwave front-end components for calibration and design purposes. Precision calibrations of microwave components require such techniques as lapping waveguide flanges (Fig. 2-23) and the use of waveguide measurement equipment components [5 (p. 15-8)]. This specialized equipment can measure waveguide components to a precision better than 0.001 dB [38]. The LNA input waveguide components require

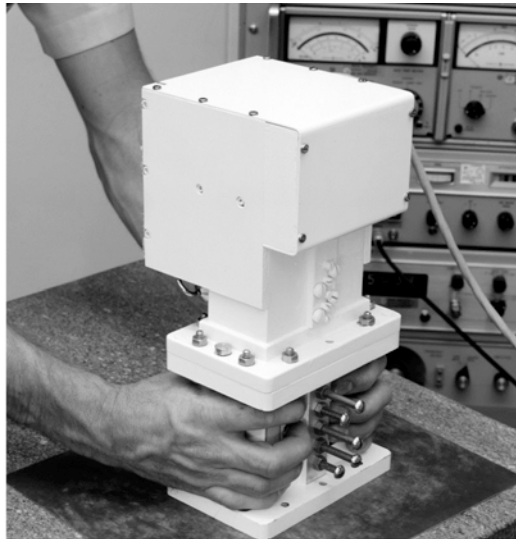


Fig. 2-23. WR430 S-band (2.295-MHz) waveguide flange lapping process for precision-insertion loss measurements.

precision waveguide flanges for best results. Assembled waveguide systems are maintained with clean, dry, pressurized gas systems. Swept-frequency insertion loss measurements over a bandwidth can be made with a commercial instrument such as the HP 8510. It is good practice to combine both measurement techniques (for both selected frequency or frequencies) with higher accuracy and a wider frequency band with less accuracy.

It is sometimes convenient to determine the loss of microwave components from measurements of a receiver effective noise temperature defined on each side of the loss. From Eq. (2.2-23), it can be shown that the insertion loss (ratio) is given by

$$L = \frac{T_p + T_{e1}}{T_p + T_{e2}} \quad (2.6-10)$$

This technique is used in Section 2.5 for calibration of the XTR feedhorn loss. Similarly, it can be shown that

$$L = \frac{T_p - T_{i1}}{T_p - T_{i2}} \quad (2.6-11)$$

2.6.3 Receiving System Nonlinearity

DSN microwave receiving systems are used for many types of noise measurements (including calibrations of antenna gain and system noise temperature T_{op}), as well as radio astronomy and radio science applications.

The accuracy of the measurements requires, among other things, knowledge or verification of the receiver-system linearity. A quantitative and proven technique [39,40], for this calibration involves the use of an ambient (for the hot) load, a non-calibrated noise diode (ND) installed at the receiver front-end (Fig. 2-24), a power meter, and a data collection system at the system output. The analysis is applicable to all types of configurations (such as “total power,” “noise adding,” and “Dicke” radiometers (discussed in Section 2.7).

Figure 2-25 shows an exaggerated nonlinear system where the input noise temperature has been increased by 50 K (turning the ND on and off) with the receiving system switched sequentially between the antenna and an ambient load. The receiver output power is compressed (solid curve) at the higher output level when switched to the ambient load so that the output reading change is less when turning the ND on and off when switched to the ambient load as compared to the antenna.

An analysis of this nonlinear system, using the linear model (dashed line) would result in incorrect noise temperature results. For example, the reading, R on the antenna, with the ND turned on, of slightly over 0.4 W would imply a

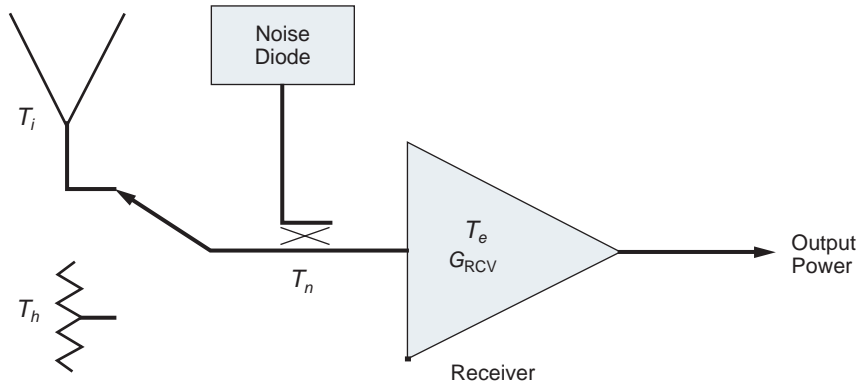


Fig. 2-24. Configuration for determining the system operating noise temperature, T_{op} , and nonlinearity by turning the noise diode on and off while switched to the antenna and the calibration load.

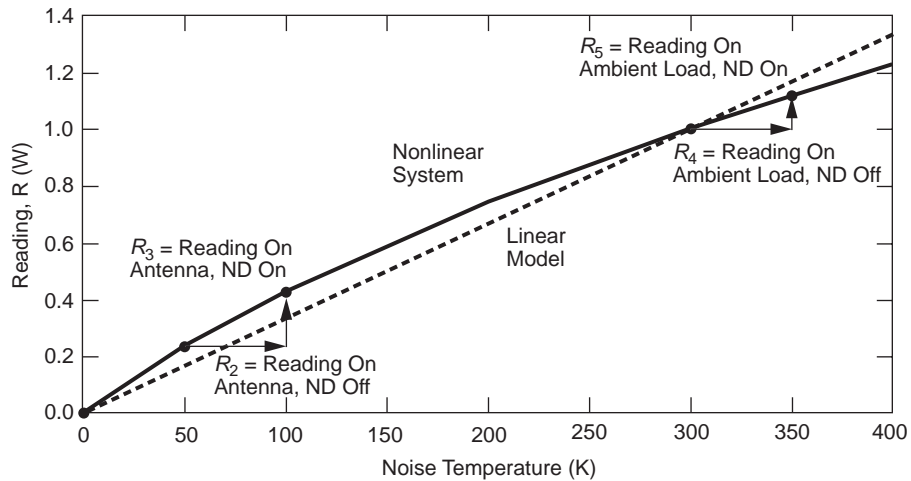


Fig. 2-25. An exaggerated receiving system nonlinearity due to gain compression (solid line) showing 50-K noise diode increase in system noise temperature with the receiver input switched to the antenna and ambient load.

noise temperature of about 125 K, an error of about 25 K (125–100). The following analysis provides the equations to quantitatively measure the degree of receiver nonlinearity and hence allow determination and maintenance of acceptable system linearity limits.

For both the linear and nonlinear model analysis, the receiving system output power readings are defined as

R_1 = power meter input terminated, W

R_2 = receiver input switched to the antenna with noise diode (ND) off, W

R_3 = same as R_2 except ND on, W

R_4 = receiver input switched to ambient load with ND off, W

R_5 = same as R_4 except ND on, W

The R_1 reading is subtracted from all subsequent readings to eliminate the power meter reading zero bias. The four remaining readings are proportional to system noise temperatures T_2 , T_3 , T_4 , and T_5 , respectively.

The linear model analysis using the bias corrected readings R_2 and R_4 has two equations of the form

$$T = BR \quad (2.6-12)$$

where

$T = T_{\text{op}}$ = receiving system operating noise temperature, K

B = receiving system linear model scale factor = T_4/R_4 , K/W

R = receiving system output power meter readings with input connected to the designated source defined for T , W

For calibration of the receiving system as a Total Power Radiometer (TPR) the LNA is switched to the hot load and the system scale factor determined from Eq. (2.6-12) (see Section 2.7)

$$B = \frac{T_4}{R_4} \quad (2.6-13)$$

where

$T_4 = T_h + T_e$ = receiving system noise temperature, with input switched to the calibration load, K

T_h = calibration load standard (usually an ambient load, with physical temperature monitored), K

$T_e = T_{\text{LNA}} + T_f$ = receiving system front-end amplifier effective input noise temperature, K

R_4 = system output power meter reading, input switched to calibration load, W

Following Eq. (2.6-12) and with Eq. (2.6-13), the system noise temperature with the receiving system input connected to the antenna is given by

$$T_{\text{op}} = T_2 = BR_2 \quad (2.6-14)$$

For this linear analysis, the evaluated noise diode noise temperatures determined by turning the noise diode on and off with input switched to the antenna or the calibration load

$$T_{n2} = T_3 - T_2 \quad (2.6-15)$$

and

$$T_{n4} = T_5 - T_4 \quad (2.6-16)$$

where

T_{n2} = noise diode noise temperature determined from linear analysis with receiver input switched to the antenna, K

T_{n4} = noise diode noise temperature determined from linear analysis with receiver input switched to the load, K

T_2 , T_3 , T_4 , and T_5 = the system noise temperatures corresponding to readings R_2 , R_3 , R_4 , and R_5 , K

If the system is nonlinear, the measured values for T_{n2} and T_{n4} will not be equal. A quadratic “corrected” solution (model) with constants B_C and C_C to be determined for the system noise temperature in terms of the linear solution T is given by

$$T_C = B_C T + C_C T^2 \quad (2.6-17)$$

where

B_C = Coefficient of the linear term for T_C , ratio ($B_C = 1$ for a perfectly linear system)

C_C = Coefficient of the quadratic term for T_C , K^{-1} ($B_C = 0$ for a perfectly linear system)

The system response to the four different states (i.e., configured to the antenna and the antenna and ambient load while the noise diode is switched on and off generates four power levels. These four power levels can be used to calculate the coefficient for the nonlinear model.

The resulting four equations are

$$T_{2C} = B_C T_2 + C_C T_2^2 \quad (2.6-18)$$

$$T_{3C} = B_C T_3 + C_C T_3^2 \quad (2.6-19)$$

$$T_4 = B_C T_4 + C_C T_4^2 \quad (\text{known calibration}) \quad (2.6-20)$$

$$T_{5C} = B_C T_5 + C_C T_5^2 \quad (2.6-21)$$

These four receiving system equations contain the nonlinear characteristics to be determined. The increase in system noise due to the injected noise of the noise diode should be equal for the antenna and ambient load configurations. The differences between T_{3C} and T_{2C} Eqs. (2.6-19 and 2.6-18) should equal the difference between T_{5C} and T_{4C} Eqs. (2.6-21 and 2.6-20). It is also known that the calibration noise temperature represented by T_4 and T_{4C} are equal and identical to the system noise temperature with the receiver input switched to the calibration ambient load ($T_{\text{op AMB}} = T_p + T_{\text{LNA}} + T_f$).

The actual differences, T_{nC} , in the two cases are equal.

$$T_{nC} = T_{3C} - T_{2C} \quad (2.6-22)$$

$$T_{nC} = T_{5C} - T_{4C} \quad (2.6-23)$$

where

T_{nC} = ND noise temperature contribution to T_{op} corrected for the receiving system nonlinearity, K

Solving the above equations, the constants B_C and C_C are given by

$$C_C = \frac{T_5 - T_4 - T_3 + T_2}{T_4(T_5 - T_4 - T_3 + T_2) - (T_5^2 - T_4^2 - T_3^2 + T_2^2)} \quad (2.6-24)$$

$$B_C = 1 - C_C T_4 \quad (2.6-25)$$

For a nearly linear receiving system, C_C approaches zero, and B_C approaches one. A receiving system “linearity factor” (FL) is defined with the receiving system connected to the antenna

$$\text{FL} = \frac{T_{2C}}{T_2} = \frac{T_{\text{op, corrected value}}}{T_{\text{op, uncorrected value}}}, \text{ ratio} \quad (2.6-26)$$

And the nonlinearity (NL) value as

$$\text{NL} = 100(\text{FL} - 1), \text{ percent} \quad (2.6-27)$$

or

$$NL = 100 \left[\frac{T_{2C}}{T_2} - 1 \right], \text{ percent} \quad (2.6-28)$$

For the ideal linear receiving system, $FL = 1$, and $NL, \text{ percent} = 0$. A DSN receiving system/radiometer system should have a measured nonlinearity magnitude of less than 0.5 percent; a goal of less than 0.2 percent is desirable. A negative NL value is due to the receiving system compressing at higher noise levels; this is the most common case. A positive NL value is explained by the receiving system gain increasing at higher noise levels; it is theorized that this could be explained by a mixer with insufficient local oscillator (LO) drive level.

Some effort has been expended looking for other curve fits than the quadratic presently used. However, the quadratic fit is well understood, it is simple to evaluate, and no advantage has been found for other models of this application with small system nonlinearity [41 (R. Unglaub, p. 15)]. The analysis is successfully performed routinely with the Goldstone antennas and is planned for all DSN antennas to monitor their noise temperature and linearity performance.

2.6.4 Receiving System Mini-cals

The equations of Section 2.6.3 are used to analyze receiving system noise temperature, linearity, and the noise diode (ND). The mini-cal data sets for this analysis consist of measurements of the receiver output power with the input switched sequentially to the antenna and calibration load (usually ambient temperature) with the ND on and off for each condition.

For example, in the Goldstone DSS-13, research 34-m antenna S-band (2.295 GHz) low noise system data set taken on 2004, day-of-year 357, the averaged system noise temperature (linear analysis) at zenith was 35.8 K (5 data points, measurement 1 sigma = 0.054 K) defined at the feedhorn aperture input. The TPR averaged linear analysis gain scale factor constant B (determined to be 3.893×10^8 K/W (measurement 1 sigma = 3.58×10^5) is used with Eq. (2.6-14) to convert the receiver output power meter readings to system noise temperature. The averaged nonlinearity was measured to be -0.44 percent (measurement 1 sigma = 0.1 percent), indicating only slight receiving system gain compression (slight since magnitude is small and compression indicated by the minus sign). The nonlinearity analysis is used to monitor the receiving system linearity performance and provides the information needed to verify, maintain, and report system performance and provide for error budget analysis. The analysis is as an aid used to modify the instrumentation and verify and report system linearity performance rather than to correct the data results for

system nonlinearity. For this example, the noise diode input defined at the feedhorn aperture was measured to be 55.95 K (measurement 1 sigma = 0.037 K).

2.7 Radiometers in the DSN

2.7.1 Introduction

DSN antennas and receivers are frequently configured for use as radiometers. Radiometers are used for DSN applications such as calibrating antenna efficiency needed to support tracking applications and for scientific applications such as planetary blackbody and “radio star” flux measurements. The antenna calibrations are performed during scheduled maintenance periods. The scientific measurements are dependent on availability of DSN antennas when they are not used for normal spacecraft tracking. The requirements for both types of measurements are similar; large stable antennas capable of operating at microwave frequencies with low system noise temperatures. Receiver linearity and amplitude stability are key issues for radiometers, although of less importance for spacecraft tracking. Well calibrated antenna and receiver systems are important for spacecraft tracking to reduce link margins and hence increase data rates and important for the scientific applications for precise results with known and reportable errors. In addition to using the DSN operational antennas for these purposes, a DSN outreach program has made an older Goldstone 34-m antenna available to the Goldstone Apple Valley Radio Telescope (GAVRT) [42] program for full-time radio astronomy use. It is expected that this program will expand to include another 34-m antenna not currently used by the DSN.

2.7.2 Total Power Radiometers

A total power radiometer (TPR) is presently available for all the DSN antenna gain measurements and system noise temperature calibrations. This is the simplest type of radiometer (Fig. 2-26) and is the standard by which other radiometers are compared [3,25]. For the TPR, from Eq. (2.6-12), the total system noise temperature is given by

$$T = BR \quad (2.7-1)$$

where

$T = T_{op}$ = system operating noise temperature, K

B = radiometer scale factor = T_4 / R_4 , K/W

R = system output reading, W

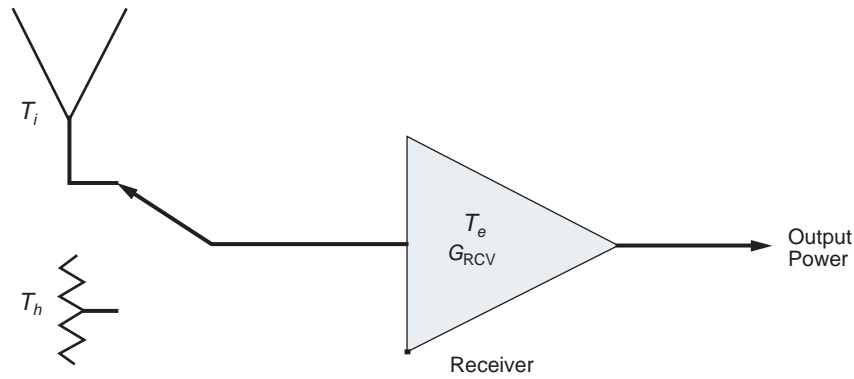


Fig. 2-26. Simplified diagram of a total power radiometer (TPR).

$T_4 = T_h + T_e =$ receiving system noise temperature, with input switched to the calibration load, K

$T_h = T_{\text{load}} =$ calibration of hot load physical temperature, K

$T_e = T_{\text{LNA}} + T_f =$ receiver effective input noise temperature, K

$R_4 =$ system output reading, input switched to calibration hot load, W

The TPR is calibrated by switching the receiver input to the calibration hot load for the determination of the radiometer scale factor B . The antenna system with a TPR can perform a variety of radio astronomy measurements. For example, the “absolute” noise measurement of an external natural radio source can be determined by pointing the antenna on and off source. The noise temperature measurement of an unknown source can be determined relative to a known source temperature. This is accomplished by measuring the increase in the maximum on-source noise temperature for both the known and unknown sources. The measurement of antenna gain and other related parameters are determined by observing a radio source with a known temperature [36]. In addition, this radiometer capability is used with natural radio sources to determine antenna pointing model performance.

The minimum detectable noise of the TPR assuming perfect gain stability, is given by [3 (p. 244)]

$$\Delta T_{\min} = \frac{T_{\text{op}}}{\sqrt{\tau B}} \quad (2.7-2)$$

where

$\Delta T_{\min} =$ minimum detectable noise, K

$T_{\text{op}} =$ system noise temperature, K

τ = radiometer integration time, seconds

B = radiometer receiving system bandwidth, Hz

Gain instability can be a serious problem for TPR measurements; more complicated radiometers circumvent this but with some degradation of the minimum ΔT_{\min} . Gain instability [3 (p. 248)] degrades the radiometer sensitivity to

$$\Delta T_{\min} = T_{\text{op}} \sqrt{\left(\frac{1}{\tau B}\right) + \left(\frac{\Delta G}{G}\right)^2} \quad (2.7-3)$$

where

$\Delta G / G$ = radiometer system gain variations, ratio

Instabilities in system noise temperature or bandwidth further decrease the radiometer sensitivity in the same manner as gain variations. Some or most of these can be improved by controlling the physical temperature of the system components. Sometimes this is best accomplished passively using thermal insulation and mass to generate a long time constant compared to the measurement time.

For characterizing the radiometer sensitivities, it is important to measure $\Delta G / G$ with respect to the environment such as the physical temperature and the amplifier's power supply voltages. This is accomplished by changing these parameters one at a time and measuring ($\Delta G / G$). This can be accomplished with the radiometer input switched to a known calibration load. In some cases it is convenient to change the physical temperature with the temperature regulator. This should be done several times noting both the temperature change and ($\Delta G / G$). Similarly, in some cases the line voltage can be changed in a controlled manner with a commercial "variac" transformer. With this information, the radiometer stability performance can be estimated for these parameters.

Radio frequency interference (RFI) within the radiometer operating bandwidth degrades radiometer performance. A site survey for RFI, radiometer equipment shielding design and fabrication and time of observation are important. Strong RFI signals outside the normal operating bandwidth can also saturate the normal power handling capabilities of LNAs and impact radiometer performance. RFI monitoring, detection, and management are important in minimizing the effect of RFI. This includes deletion of corrupted data and (if necessary) rescheduling observations.

2.7.3 Dicke Radiometers

Dicke [3 (p. 248)] radiometers (Fig. 2-27) are used in the radio astronomy community to reduce the effect of receiver gain instability by continuously

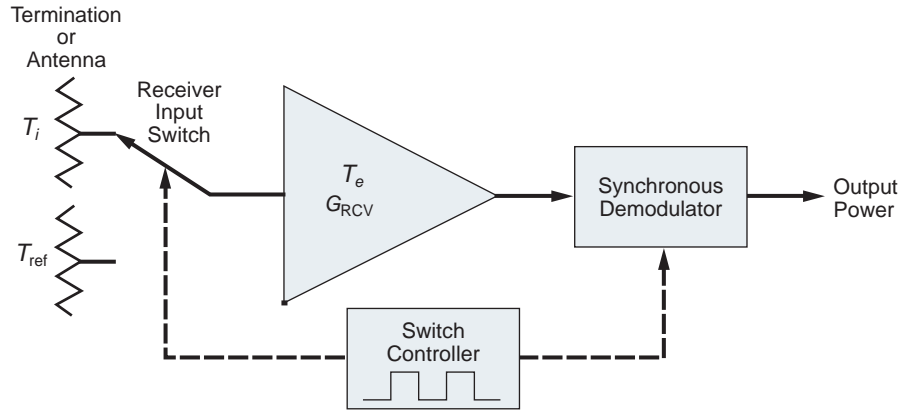


Fig. 2-27. Simplified diagram of a Dicke radiometer.

switching the receiver input between the antenna and a reference load. These are not used in the operational DSN due to compromising the receiving system when switched to the reference load. In addition, the typically higher resistive loss of a fast waveguide switch compared to the specially designed DSN low-loss waveguide switches used in the microwave front-end is incompatible with a very low system noise temperature (0.01 dB loss contributes ~ 0.67 K noise temperature, see Section 2.6.2).

The sensitivity of a basic "balanced" (reference load (T_{ref}) and antenna noise (T_i) temperatures equalized, square wave multiplication and modulation) Dicke radiometer optimum performance is given by twice the value for a TPR [3 (pp. 248, 258)]

$$\Delta T_{\min} = 2 \frac{T_{op}}{\sqrt{\tau B}} \quad (2.7-4)$$

The DSN Goldstone 70-m antenna research feedcone is equipped with a K-band (22-GHz) beam-switching radiometer configuration using two feedhorns useful for radio astronomy applications. This has the advantage of the Dicke concept, using the second feed as the reference load, thus obtaining the performance of a balanced Dicke radiometer. An added advantage is that atmospheric instabilities are largely canceled since the two feedhorns "see" nearly identical regions of the sky.

2.7.4 Noise-Adding Radiometers

The DSN uses "noise-adding" radiometers (NARs) operationally for monitoring system noise temperature during spacecraft tracking (Fig. 2-28). The injected noise from a noise diode is small compared to the system noise

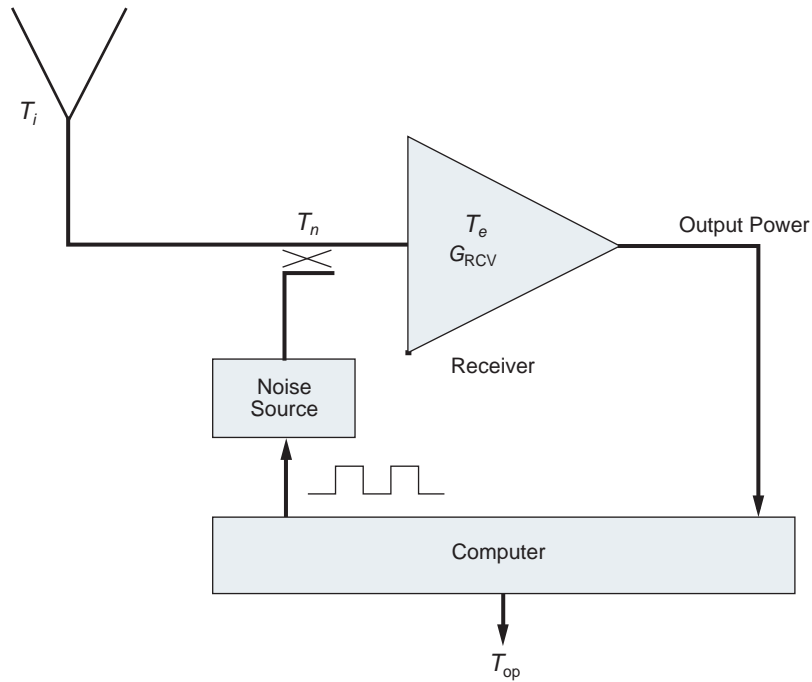


Fig. 2-28. Simplified diagram of a noise adding radiometer (NAR).

temperature (T_{op}) to minimize the impact on the system noise temperature and the modulated telemetry signals.

For the application of radio astronomy observations, antenna calibrations, and system performance measurements the injected noise from a noise diode needs to be large compared to the system noise temperature (T_{op}) to improve the measurement resolution. To satisfy all applications of the NAR, multiple noise diode levels are required.

The NAR Y -factor (with the receiving system switched to the antenna) with the noise diode pulsing on and off is given by

$$Y_n = \frac{T_{op} + T_n}{T_{op}} \quad (2.7-5)$$

where

$Y_n = P_{non} / P_{noff} =$ noise diode on and off Y -factor, ratio

$T_n =$ noise diode temperature contribution at the input of the receiving system, K

The technique for calibrating the noise diode as required for measuring the system noise temperature depends on the calibration load; if T_e is known, switching the receiver to the calibration hot (usually ambient) load provides a known system temperature, T_{opload} ; solving Eq. (2.7-5) for T_n with this condition and measuring Y_n

$$T_n = T_{\text{opload}}(Y_n - 1) \quad (2.7-6)$$

where

$T_{\text{opload}} = (T_{\text{pload}} + T_e) =$ system noise temperature with the LNA connected to the hot (ambient) calibration load, K

$T_h = T_{\text{pload}} =$ physical temperature of the ambient calibration hot load, K

$T_e =$ receiving system noise temperature, K

An alternate method is to perform “mini-cals” (Section 2.6.4) in the TPR mode with the antenna at zenith, measuring system linearity and other parameters as well as the calibration of the noise diode, T_n . Then use the noise diode for the NAR. The noise diode is best evaluated relative to the antenna (T_{2n}) instead of relative to the hot load (T_{4n}) due to the higher measurement scatter on the hot load.

With T_n calibrated and continuously measuring Y_n , the NAR provides a measurement of system noise temperatures

$$T_{\text{op}} = \frac{T_n}{Y_n - 1} \quad (2.7-7)$$

The NAR radiometer noise temperature measurement resolution for equal on and off periods is given by [35; 5 (p. 19-1)]

$$\Delta T_{\text{min}} = \frac{2T_{\text{op}}}{\sqrt{\tau B}} \left(1 + \frac{T_{\text{op}}}{T_n} \right) \quad (2.7-8)$$

Inspection of Eq. (2.7-8) reveals that ΔT_{min} is optimized with large values for T_n . This is not an option for use during tracking spacecraft due to the increase in T_{op} . However, for radio astronomy and other applications, it is desirable to use a large value for T_n . With high values of T_n , $(T_{\text{op}}/T_n) \ll 1$, the NAR sensitivity performance approaches that of a Dicke radiometer.

However, there is a limit for high values of T_n due to saturation of the receiver amplifier(s) (Section 2.6.4). Eq. (2.7-8) neglects some sources of instability such as the noise diode itself. The noise diode should be temperature and current stabilized [17]. Low-loss microwave couplers are used for the noise diode coupling to the receiving system input, minimizing increased system noise temperature associated with this radiometer capability. The advantage of the NAR for the DSN is that the effects of gain instability are largely eliminated as compared with the TPR.

The external influences for the NAR are mostly transferred from the stability of the amplifiers to the stability of the noise diode. Expanding Eq. (2.7-8) to account for this,

$$\Delta T_{\min} = T_{\text{op}} \sqrt{\left(\frac{4}{\tau B}\right) \left(1 + \frac{T_{\text{op}}}{T_n}\right)^2 + \left(\frac{\Delta T_n}{T_n}\right)^2} \quad (2.7-9)$$

where

$$\Delta T_n / T_n = \text{noise diode instability, ratio}$$

The stability performance for the NAR depends on the noise diode stability instead of the system gain stability.

The system noise temperature for a typical DSN antenna configuration is monitored with the NAR during normal operational tracking of a spacecraft. In this case T_n is usually made quite small, on the order of 0.25 to 1 K to minimize the increase of system noise temperature. This requires a larger number of samples, with a longer total integration time to obtain a suitable measurement resolution. However, longer integration time is limited due to dynamic changes in noise temperature with elevation angle and other effects.

2.7.4.1 Noise Diode Duty Cycle. The NAR performance is analyzed using unequal noise diode on-and-off periods. Treating the noise diode on-and-off periods separately in the NAR Eq. (2.7-7) each with an independent delta noise temperature appropriate for a TPR

$$\begin{aligned} (\Delta T_{\text{op}})^2 = & \left(\frac{\partial T_{\text{op}}}{\partial P_{\text{noff}}}\right)^2 (\Delta P_{\text{noff}})^2 \\ & + \left(\frac{\partial T_{\text{op}}}{\partial P_{\text{non}}}\right)^2 (\Delta P_{\text{non}})^2 \end{aligned} \quad (2.7-10)$$

where

P_{noff} = radiometer output power with noise diode off, W

P_{non} = radiometer output power with noise diode on, W

For a single switching cycle

$$\begin{aligned} (\Delta T_{op})^2 = & \left(\frac{T_{op} P_{non}}{P_{noff} (P_{non} - P_{noff})} \right)^2 \frac{P_{noff}^2}{\tau_1 B} \\ & + \left(\frac{T_{op}}{(P_{non} - P_{noff})} \right)^2 \frac{P_{non}^2}{\tau_2 B} \end{aligned} \quad (2.7-11)$$

where

τ_1 = time during the NAR cycle period that noise diode off, s

τ_2 = time during the NAR cycle period that the noise diode on, s

Collecting terms and using

$$\frac{P_{non}}{P_{non} - P_{noff}} = \left(1 + \frac{T_{op}}{T_n} \right) \quad (2.7-12)$$

For 1 cycle

$$\Delta T_{min} = T_{op} \left(1 + \frac{T_{op}}{T_n} \right) \frac{\sqrt{\left[\frac{1}{\tau_1} + \frac{1}{\tau_2} \right]}}{\sqrt{B}} \quad (2.7-13)$$

For multiple cycles with total integration time τ

$$\Delta T_{min} = m T_{op} \frac{\left(1 + \frac{T_{op}}{T_n} \right)}{\sqrt{\tau B}} \quad (2.7-14)$$

where

m = NAR ΔT_{min} multiplier

= $\Delta T_{min}(F) / \Delta T_{min}(F = 0.5)$

= $\sqrt{1/(F(1-F))}$ (obtained by setting Eq. (2.7-13) = Eq. (2.7-14) with $\tau = p$), ratio.

F = fraction of the cycle period time with noise diode on, ratio

$\tau_1 = (1-F)p$ = time during the NAR cycle period with noise diode off, s

$\tau_2 = Fp$ = time during the NAR cycle period with the noise diode on, s

$p = (\tau_1 + \tau_2)$ = cycle period, s

τ = total integration time allowing for multiple cycles, s

Figure 2-29 shows a plot of m , the NAR ΔT_{\min} multiplier as a function of F . The optimum performance (minimum value for ΔT_{\min}) is obtained for $F = 50$ percent, equal noise diode on-and-off times, in agreement with Eq. (2.7-8). For 10-percent on-time, m is increased from 2 to 3.33 (67 percent).

2.7.5 Radiometer Stability Performance

System gain stability is one of the most important parameters for a radiometer; a sequence of output power readings from the receiver provides

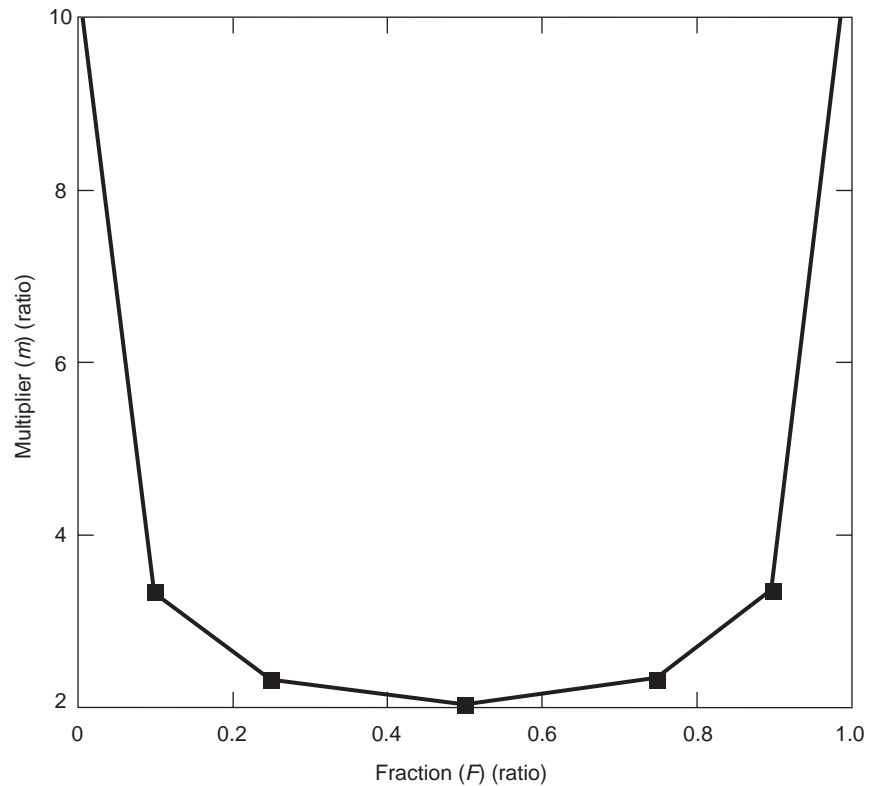


Fig. 2-29. Computation of the noise adding radiometer (NAR) ΔT_{\min} multiplier m as a fraction of the time the noise diode is turned on during an on-off cycle; 50 percent is optimal.

data for this estimate. Since the thermal noise power available from a load is given by $P = kTB$, the system gain is given by

$$G = \frac{R_4}{kT_4B} \quad (2.7-15)$$

where

G = system gain, ratio

R_4 = system output power reading, W

T_4 = system noise temperature when the receiver amplifier input switched to the calibration load, K

k = Boltzmann's constant = 1.38065×10^{-23} J/K

B = BW = system bandwidth, Hz

The physical temperature of the calibration load combined with the amplifier output power readings provides a useful technique for measuring system gain stability. Figure 2-30 shows analysis results of measurements with the Goldstone DSS 12 (GAVRT) 34-m antenna receiving system operating at X-band (8.420 GHz) on 2006, DOY 270 (September 27, 2006). Plot (a) shows a plot of the input thermal noise power ($P = kT_4B$) relative to the first reading (ratio) and output measured power (R_4) relative to the first reading (ratio) over time combined to calculate the receiving system gain using Eq. (2.7-15) over the same time. This calculation accounts for the changing input power with the measured physical temperature of the calibration load. The gain is reduced by ~0.5 dB over ~5 hours or about 0.1 dB/hr. This was during a physical temperature change of about 9.4 C. It is presumed that the gain change will be reduced during periods of more stable environmental temperatures. This can be achieved with improved temperature control of the system components.

To accommodate gain changes, either frequent mini-calibrations (mini-cals) are helpful, or another configuration is required (such as the NAR). In cases where the noise diode (ND) is more stable than the receiver gain (G), the NAR solution will compensate and could provide the "better" system performance depending on the application requirements and system parameters.

2.8 Status and Future

The science and art of calibrating low-noise receiving systems for the DSN large antennas has been maturing for many years, and will continue to improve in the future. Over the years of the DSN's existence, problems and uncertainties with precision calibrations have been overcome. For example, the DSN has developed, tested, and implemented convenient quantitative methods for

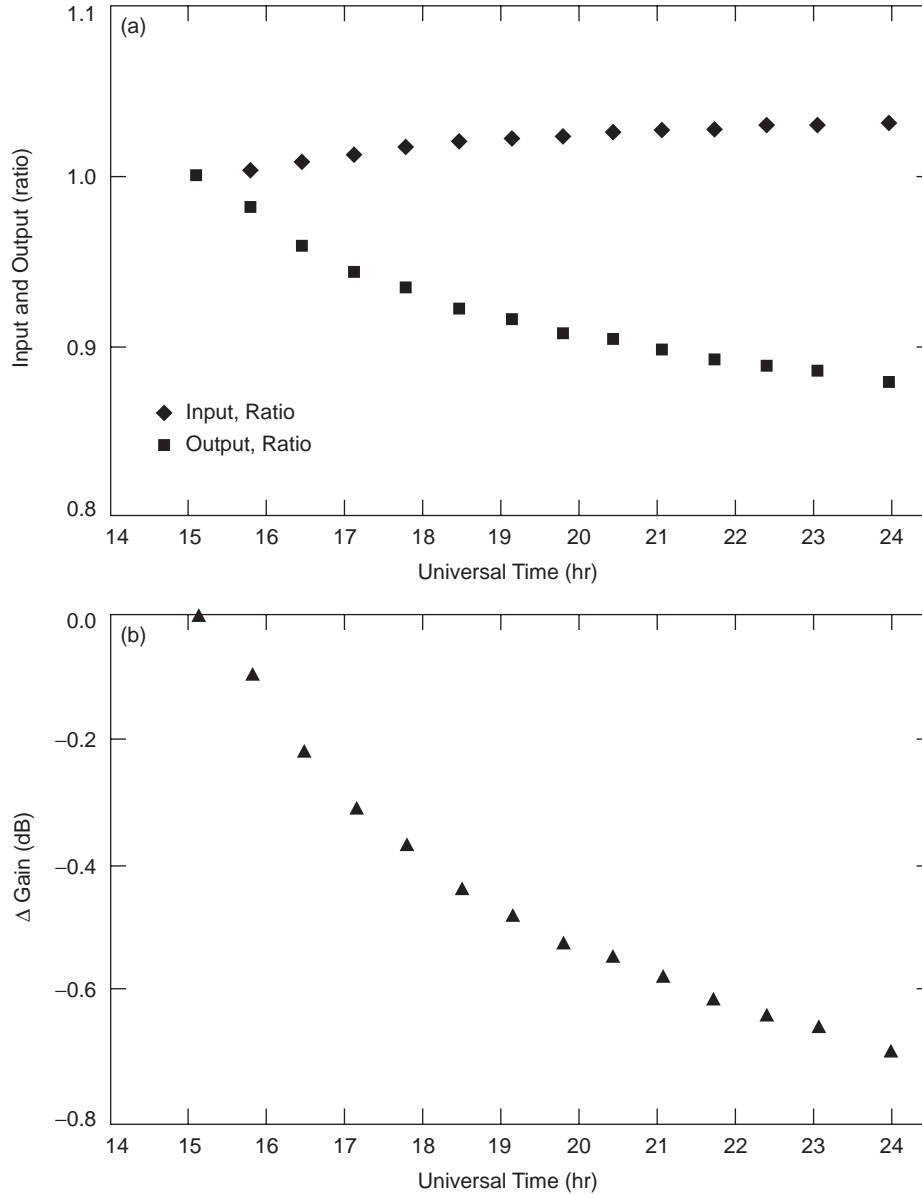


Fig. 2-30. Analysis of Goldstone DSS 12 (GAVRT) 34-m antenna receiving system operating at X-band: (a) input (kT_dB) and output (R_d) changes over time and (b) gain (R_d/kT_dB) change over time.

verifying system linearity. New receiving system feedcones are now calibrated using a tested and agreed-upon sequence of measurements both on the ground and on the antenna. Each antenna system noise temperature is measured and verified periodically using a simple ambient calibration load and power meter.

The theory for these techniques is understood, shared, and coordinated throughout the DSN, often by microwave workshops for engineers and technicians at all DSN locations.

The DSN will continue to make improvements in calibrations and standardization, instrumentation hardware, error analysis, training, and documentation and reporting. The large number of remotely located antennas in the DSN requires diligence in providing future missions with timely and accurate ground station performance data. These are needed for system design, future mission planning, and commitments to optimize data transfer rates between the spacecraft and the worldwide multiple frequency ground antenna systems. This suggests improved automation for calibrating system noise temperature in the DSN antenna systems. These calibrations are essential for validating requirements and also for reducing costs.

In order to meet the higher data rate requirements for deep space tracking in the future, the DSN will develop, implement, and operate large arrays of antennas. These will require sophisticated calibration and operation procedures. The arrays of antennas with lower implementation, operation, and maintenance costs per antenna will result in different constraints and techniques not reflected in this chapter.

Possible improvements for DSN low-noise receiving systems include:

- 1) Improve the accuracy and calculation convenience for estimating the increase in DSN antennas system noise temperature due to the contributions of the Sun, Moon, planets, and radio sources both near and within each DSN antenna's main beam. This should include sources with solid angles from small to large compared with the antennas solid-angle beamwidth.
- 2) Improve the accuracy for DSN antennas system noise temperature specifications of T_{AMW} at low elevation angles ($6 \text{ deg} < T_{AMW} < 15 \text{ deg}$) for all DSN antennas at all DSN communications frequencies.
- 3) Improve and simplify calibrating techniques for the DSN LNAs at JPL and at the DSN antenna sites, including
 - a) Provide LNA noise temperature calibration techniques on the antenna
 - b) Provide simplified and accurate noise temperature calibration techniques for the antenna accounting for the atmosphere independent of a water vapor radiometer (WVR).

Challenges for the DSN for future improvements in noise temperature calibrations and standardization include

- 1) Continuing the worldwide coordination and improvements of noise temperature calibration techniques and standards for the DSN high G/T antenna systems
- 2) More and improved automation

- 3) New concepts and methods for future arrayed antenna systems
- 4) Improve and expand the radio source list for antenna calibrations [36]

Notation and Terms

2005-320 = year-day of year (DOY) date notation example

A = attenuation, dB

A_{atm} = propagation attenuation through the atmosphere, dB

$A_{\text{atm}1,2}$ = propagation attenuation through the atmosphere at elevation angles 1 or 2, dB

$A_{\text{atm}Z}$ = propagation attenuation through the atmosphere at zenith, dB

A_e = antenna effective area, m^2

A_{feed} = feed assembly attenuation, dB = $10^{(L_{\text{feed}} \cdot \text{ratio}/10)}$

AM = Air Mass = equivalent to 1 atmosphere, ratio

AMW = combined antenna and microwave system

A_p = antenna physical area, m^2

A_{std} = $10 \log L_{\text{std}}$, dB

B = BW = noise bandwidth, Hz

B = TPR linear model scale factor, K/W

B_C = coefficient (= 1 for a perfect linear system) of the linear term for T_C , ratio

C_C = coefficient (= 0 for a perfect linear system) of the quadratic term for T_C , K^{-1}

CMB = Cosmic Microwave Background

CMF = Cosmic Microwave Foreground

D_e = antenna effective diameter, m

del = Δ

D_p = antenna physical diameter, m

$\Delta G / G$ = receiving system gain instability, ratio

ΔT_{min} = minimum detectable noise level, K

$\Delta T_n / T_n$ = noise diode instability, ratio

EL = antenna elevation angle, deg

$EL_{1,2}$ = antenna elevation angle 1 or 2, deg

ε = antenna gain efficiency (less than 1), ratio

f = operating frequency, Hz

F = function of the cycle period with noise diode on, ratio

feed assembly = feedhorn + ambient waveguide components

front-end assembly = feed assembly + LNA assembly

$FL = T_{2C} / T_2$ = receiving system linearity factor (= 1 for a perfect linear system), ratio

G = available power gain, ratio

G_i = antenna gain relative to isotropic radiator, ratio (G_i , dB = 10 log G_i)

G_m = maximum available power gain, ratio

G_n = gain of amplifier n of cascaded amplifiers, ratio

h = Planck's constant = 6.626069×10^{-34} , Js

HPBW = half-power beam width of antenna pattern main beam, deg

J = joule

k = Boltzmann's constant = 1.38065×10^{-23} , J/K

K = kelvin

L = loss, ratio

λ = wavelength, m

L_{atm} = atmospheric loss, ratio

$L_{\text{atm}1,2}$ = atmospheric loss, at elevation angles 1 or 2, ratio

$L_{\text{atm}Z}$ = atmospheric loss at zenith, ratio

L_{ATT} = adjustable attenuator located between the post amplifier output and the downconverter input for system gain "level set," ratio

L_{feed} = feed assembly loss, ratio

LNA = low-noise amplifier

LNA Assembly = LNA + post amplifier + gain set attenuator

L_{std} = loss of calibrated standard (std) feedhorn used with the LNA noise temperature calibration defined from the feedhorn aperture to the LNA input, ratio

m = NAR ΔT_{min} multiplier, ratio

$M = G/T$ = receiving system performance figure of merit in terms of antenna gain (relative to isotropic radiator and receiving system operating noise temperature (relative to 1 K), ratio (M , dB = $10 \log M$)

N_a = noise power density delivered by the antenna into a matched termination, W/Hz

ND = noise diode

NL = $100 (FL - 1)$ = receiving system nonlinearity, percent

N_o = amplifier output noise power, W

$p = (\tau_1 + \tau_2)$ = NAR ND cycle period, seconds (τ_1 = ND off time, τ_2 = ND on time)

P_h / P_a = hot (ambient) load and antenna Y-factor, ratio

P_h / P_c = hot (ambient) and cold loads Y-factor, ratio

P_{LNAoff} = receiver output power with LNA off, W

P_{LNAon} = receiver output power with LNA on, W

P_{noff} = receiver output power with ND off, W

P_{non} = receiver output power with ND on, W

P_o = receiver output noise power, W

$Q = (\Delta T_{op} - \Delta T_{ant}) / (T_{patm} - T_{CMB})$ = constant used in the quadratic solution of atmospheric loss, ratio

$R_1, R_2, R_3, R_4,$ and R_5 = power meter readings associated with receiving system $T_1, T_2, T_3, T_4,$ and T_5 temperatures, W

Rayleigh-Jeans (R-J) = source noise temperature approximated by the source physical temperature, K

s = second

S_e = LNA input VSWR, ratio

SEP = Sun–Earth–Probe offset angle

S_p = calibration load input VSWR, ratio

SPD = S-band polarization diversity (feedcone)

std = standard

τ = NAR total integration time normally consisting of numerous cycles, seconds

$T = T_2 = T_{op}$, K

$T_1, T_2, T_3, T_4,$ and T_5 = radiometer system operating noise temperatures using linear equations, K

T_1 = power meter input terminated in ambient termination, K

$T_2 = T_{Op}$ = system operating noise temperature with LNA connected to antenna and ND off, K

T_3 = same as T_2 except ND on, K

T_4 = system operating noise temperature with LNA connected to calibration load with ND off, K

T_5 = same as T_4 = except ND on, K

$T_{2C} = T_{Op}$ corrected for nonlinearity, K

$T_a = T_{ant} = N_a / k$ = antenna noise temperature, K

$T_{AMW} = T_{ant} + T_{feed} + T_{LNA} + T_f$ = antenna microwave system noise temperature, K

T_{ant} = antenna noise temperature, K

T_{atm} = noise temperature of the atmosphere, K

T_c = physical temperature of the cold load, K

T_C = corrected receiving system noise temperature in terms of the linear solution, K

T_{CMB} = Cosmic Microwave Background noise temperature, K

T_{cryo} = LNA cryo system physical temperature, K

T_{DC} = down converter input noise temperature, K

T_e = receiver effective input noise temperature, K

$T_{e1,2}$ = receiver effective input noise temperature, defined at reference locations 1 or 2, K

T_{en} = effective input noise temperature of amplifier n of cascaded amplifiers, K

T_f = follow-up amplifier noise temperature, K

T_F = follow-up amplifier noise temperature defined at its input, K

T_{f1} = follow-up amplifier noise temperature defined feedhorn aperture, K

T_{f2} = follow-up amplifier noise temperature defined LNA input, K

- T_{feed} = noise temperature of the feed assembly, K
- T_h = physical temperature of the hot (ambient) load, K
- T_i = receiving system input noise temperature, K
- $T_{i1,2}$ = receiving system input noise temperature at reference locations 1 or 2, K
- T_k = blackbody disk temperature of the planet, K
- $T_{L1} = (L-1)T_p$ = loss noise temperature at reference location 1, K
- $T_{L2} = (1-1/L)T_p$ = loss noise temperature at reference location 2, K
- T_{LNA} = LNA noise temperature, K
- $T_{\text{LNA}1,2}$ = LNA noise temperature at reference locations 1 and 2, K
- $T_{\text{load}} = T_h = T_{\text{amb}}$ = physical temperature of the hot (ambient) load, K
- T_n = ND noise temperature contribution to T_{op} when turned on, K
- T_{n2} = ND noise temperature contribution to T_{op} (LNA input connected to antenna) when turned on, K
- T_{n4} = ND noise temperature contribution to T_{op} (LNA input connected to ambient load) when turned on, K
- T_{nC} = ND noise temperature contribution to T_{op} corrected for system nonlinearity, K
- $T_{\text{op}} = T = T_{\text{sky}} + T_{\text{AMW}}$ = system operating noise temperature, K
- * $T_{\text{op}1,2}$ = system operating noise temperatures at antenna elevation angles 1 or 2, K
- * $T_{\text{op}1,2,3}$ = system operating noise temperatures at reference locations 1, 2, or 3, K
- $T_{\text{op}90,30}$ = system noise temperature at elevation angles 90 and 30 degrees, K
- $T_{\text{opamb}} = T_{\text{opload}} = (T_{p\text{amb}} + T_e) = T_{p\text{load}} + T_e$ = system noise temperature with the LNA connected to the hot (ambient) calibration load, K
- $T_p = T_{\text{phy}}$ = physical temperature of the calibration load and the feed assembly, K

* $T_{\text{op}1,2}$ = can be either elevation or reference location depending on the context.

T_{patm} = equivalent physical temperature of the atmosphere, K

T_{pl} = increased system noise temperature due to a planet in the antenna beam, K

T_{P1} = source noise temperature with Planck's radiation law correction, K

T_{pload} = physical temperature of the load, K

T_{ref} = Dicke radiometer reference termination, K

$T_s = P_s / kB$ = signal source equivalent noise temperature contribution to the receiver input, K

$T_{sky} = T_{atm} + T_{CMB} / L_{atm}$ = sky noise temperature due to the atmosphere and CMB, K

$T_{UWV} = T_{e1}$ = microwave receiver effective input noise temperature, defined at feedhorn aperture, K

θ / θ_0 = angle between planet and antenna beam centers relative to the antenna HPBW, ratio

VSWR = voltage standing wave ratio, ratio

WVR = water vapor radiometer

$x = hf/kT$, ratio

XKR = X-band/K-band radar (feedcone)

XTR = X-band transmit/receive (feedcone)

$Y_{ah} = P_h / P_a$ = hot (ambient) load and antenna Y-factor, ratio

$Y_{ch} = P_h / P_c$ = hot (ambient) and cold load Y-factor, ratio

$Y_n = P_{non} / P_{noff}$ = noise diode on and off Y-factor, ratio

$Y_{oo} = P_{LNAon} / P_{LNAoff}$ = LNA on and off Y-factor, ratio

Z = zenith

References

- [1] CCIR, "Worldwide Minimum External Noise Levels, 0.1 Hz to 100 GHz," Report 670, Comité Consultatif International des Radio Communications (French: International Radio Consultative Committee) (CCIR) XIV Plenary Assembly, Kyoto, Japan, Vol. I, International Telecommunications Union (ITU), Geneva, Switzerland, 1978, pp. 422–427.

- [2] W. Flock and E. Smith, "Natural radio noise—A mini-review," *IEEE Transactions on Antennas and Propagation*, vol. 32, issue 7, pp. 762–767, July 1984.
- [3] J. D. Kraus, *Radio Astronomy*, McGraw-Hill Book Company, New York, New York, 1966.
- [4] W. W. Mumford and E. H. Scheibe, *Noise; Performance Factors in Communication Systems*, Horizon House–Microwave, Inc., Dedham, Massachusetts, 1968.
- [5] C. T. Stelzried, *The Deep Space Network – Noise Temperature Concepts, Measurement, and Performance*, JPL Publication 82-33, Jet Propulsion Laboratory, Pasadena, California, September 1982.
- [6] A. A. Penzias and R. W. Wilson, "A Measurement of Excess Antenna Temperature at 4080 Mc/s," *The Astrophysical Journal*, vol. 142, no. 1, July 1965, pp. 419–421.
- [7] J. C. Mather, D. J. Fixsen, R. A. Shafer, C. Mosier, and D. T. Wilkinson, "Calibrator Design for the COBE Far Infrared Absolute Spectrophotometer (FIRAS)," *The Astrophysical Journal*, vol. 512, pp. 511–520, February 20, 1999.
- [8] A. Olivieria-Costa and M. Tegmark, editors, *Microwave Foregrounds: Astronomical Society of the Pacific Series*, Vol. 181, San Francisco, California, 1999.
- [9] J. D. Johnson, "Thermal Agitation of Electricity in Conductors," *Physical Review*, vol. 32, no.1, pp. 97–109, July 1928.
- [10] H. Nyquist, "Thermal Agitation of Electric Charge in Conductors," *Physical Review*, vol. 32, no. 1, pp. 110–113, July 1928.
- [11] *IEEE 100: The Authoritative Dictionary of IEEE Standards Terms*, 7th ed., The Institute of Electrical and Electronics Engineers, Inc., New York, New York, December 2000.
- [12] "IRE Standards on Electron Tubes: Definitions of Terms, 1962 (62 IRE 7.S2)," *Proceedings of the IEEE*, vol. 51, pp. 434–435, March 1963.
- [13] T. Y. Otoshi, "Antenna System Noise-Temperature Calibration Mismatch Errors Revisited," *The Interplanetary Network Progress Report 42-148, October–December 2001*, Jet Propulsion Laboratory, Pasadena, California, pp. 1–31, February 15, 2002.
http://ipnpr.jpl.nasa.gov/progress_report/
- [14] J. Layland and L. Rauch, "The Evolution of Technology in the Deep Space Network: A History of the Advanced Systems Program," *The Telecommunications and Data Progress Report 42-130, April–June 1997*, Jet Propulsion Laboratory, Pasadena, California, pp. 1–44, August

- 15, 1997, (also available as JPL publication 95-20 at <http://tmot.jpl.nasa.gov/>, click on Program Overview Information). http://ipnpr.jpl.nasa.gov/progress_report/
- [15] W. A. Imbriale, *Large Antennas of the Deep Space Network*, John Wiley and Sons, Hoboken, New Jersey, 2003.
- [16] C. T. Stelzried, G. S. Levy, and M. S. Katow, "Multi-feed Cone Cassegrain Antenna," U.S. Patent 3,534,375, October 13, 1970.
- [17] K. B. Wallace, "Noise Diode Evaluation," JPL Technical Report, 22-1526, Vol. 3, p. 121, April 15, 1973.
- [18] C. T. Stelzried, R. C. Clauss, and S. M. Petty, "Deep Space Network Receiving Systems' Operating Noise Temperature Measurements," *The Interplanetary Network Progress Report 42-154, April–June 2003*, Jet Propulsion Laboratory, Pasadena, California, pp. 1–7, August 15, 2003. http://ipnpr.jpl.nasa.gov/progress_report/
- [19] H. Dwight, *Tables of Integrals and Other Mathematical Data*, 4th ed, 9th printing, The Macmillan Company, New York, New York, 1968.
- [20] W. V. T. Rusch and P. D. Potter, *Analysis of Reflector Antennas*, Academic Press, New York, New York, 1970.
- [21] T. Y. Otoshi, "Noise Temperature Due to Reflector Surface Resistivity," *The Interplanetary Network Progress Report 42-154, April–June 2003*, pp. 1–13, August 15, 2003. http://ipnpr.jpl.nasa.gov/progress_report/
- [22] T. Y. Otoshi, Y. Rahmat-Samii, R. Cirillo, Jr., and J. Sosnowski, "Noise Temperature and Gain Loss due to Paints and Primers on DSN Antenna Reflector Surfaces," *Telecommunications and Mission Operations Progress Report 42-140*, October–December 1999, Jet Propulsion Laboratory, Pasadena, California, pp. 1–26, February 15, 2000. http://ipnpr.jpl.nasa.gov/progress_report/
- [23] T. Y. Otoshi and M. M. Franco, "Radiometric Tests on Wet and Dry Antenna Reflector Surface Panels," *The Telecommunications and Data Progress Report 42-100, October–December 1989*, Jet Propulsion Laboratory, Pasadena, California, pp. 111–130, February 15, 1990. http://ipnpr.jpl.nasa.gov/progress_report/
- [24] *DSMS Telecommunications Link Design Handbook*, 810-005, Rev. E, JPL D-19379 (JPL internal document that has been cleared for external release), Jet Propulsion Laboratory, Pasadena, California, modular document with initial release of Rev. E, January 15, 2001 with ongoing updates. <http://eis.jpl.nasa.gov/deepspace/dsndocs/810-005/>
- [25] R. S. Colvin, *A Study of Radio-Astronomy Receivers*, Publication No. 18A, Stanford Radio Astronomy Institute, Stanford, California, October 31, 1961.

- [26] J. R. Pierce and E. C. Posner, *Introduction to Communication Science and Systems*, Plenum Press, New York, New York, 1980.
- [27] D. Bathker and D. Brown, "Large Ground Antenna Performance with Solar Noise Jamming," *Proceedings of the IEEE*, vol. 54, issue 12, pp. 1949–1951, December 1966.
- [28] I. de Pater, "Radio Images of the Planets," *Annual Review of Astronomy and Astrophysics*, vol. 28 (A91-28201 10-90) Palo Alto, California, Annual Reviews, Inc., pp. 347–399, 1990.
<http://www.annualreviews.org/>
- [29] A. V. Kantak and S. D. Slobin, *System Noise Temperature Increase from the Sun, Moon, or Planet Blackbody Disk Temperature*, JPL D-33697 (JPL internal document), Jet Propulsion Laboratory, Pasadena, California, December 2005.
- [30] J. Bautista, R. Clauss, S. Petty, and J. Shell, "DSN Low Noise Amplifiers in the New Millennium," *TMOD Technology and Science Program News*, Issue 13, Rev. 1, Jet Propulsion Laboratory, Pasadena, California, January 2001.
http://tmot.jpl.nasa.gov/Program_Overview_Information/IND_Program_News/ind_program_news1.html
- [31] D. F. Wait, "Satellite Earth Terminal G/T Measurements," *Microwave Journal*, vol. 20, no. 4, pp. 49, 51, 58, April 1977.
- [32] N. A. Renzetti, *The Deep Space Network—A Radio Communications Instrument for Deep Space Exploration*, JPL Publication 82-104, Jet Propulsion Laboratory, Pasadena, California, July 1983.
- [33] P. H. Stanton, D. J. Hoppe, and H. Reilly, "Development of a 7.2-, 8.4-, and 32-Gigahertz (X-/X-/Ka-Band) Three-Frequency Feed for the Deep Space Network," *The Telecommunications and Mission Operations Progress Report 42-145, January–March 2001*, Jet Propulsion Laboratory, Pasadena, California, pp. 1–20, May 15, 2001.
http://ipnpr.jpl.nasa.gov/progress_report/
- [34] Yardley Beers, *Introduction the Theory of Error*, Second Edition, Addison-Wesley Publishing Company, Menlo Park, California, June 1962.
- [35] P. D. Batelaan, R. M. Goldstein and C. T. Stelzried, "A Noise-Adding Radiometer for Use in the DSN," *DSN Space Programs Summary 37-65*, Vol. 2, pp. 66–69, Jet Propulsion Laboratory, Pasadena, California, September /30, 1970.
- [36] P. Richter, "Radio Source List for Antenna Calibration," DSN No. 890-269, JPL D-3801 (JPL internal document), Jet Propulsion Laboratory, Pasadena, California, October 15, 1994.

- [37] C. T. Stelzried, "Operating Noise-Temperature Calibrations of Low-Noise Receiving Systems," *Microwave Journal*, vol. 14, pp.41–48, June 1971.
- [38] C. T. Stelzried, M. S. Reid, and S. M. Petty, "A Precision DC Potentiometer Microwave Insertion Loss Test Set," *IEEE Transactions on Instrumentation and Measurement*, IM-15, pp. 98–104, March 1966.
- [39] C. T. Stelzried and M. J. Klein, "Precision DSN Radiometer Systems: Impact on Microwave Calibrations," *Proceedings of the IEEE*, vol. 82, no. 5, pp. 636–645, May 1994.
- [40] C. T. Stelzried and M. J. Klein, Corrections to "Precision DSN Radiometer Systems: Impact on Microwave Calibrations," *Proceedings of the IEEE*, vol. 84, no. 8, p. 1187, August 1996.
- [41] A. Freiley, C. Stelzried, R. Unglaub, *Microwave Radiometer System Performance including Linearity Verification*, JPL D-31547 (JPL internal document), Jet Propulsion Laboratory, Pasadena, California, February 28, 2005.
- [42] D. F. Miller, *Basics of Radio Astronomy for the Goldstone-Apple Valley Radio Telescope*, JPL Document D-13835 (JPL internal document), Jet Propulsion Laboratory, Pasadena, California, April 1998.
<http://www.jpl.nasa.gov/radioastronomy>
- [43] D. A. Bathker, W. Veruttipong, T. Y. Otoshi, and P. W. Cramer, Jr., "Beam-Waveguide Antenna Performance Predictions with Comparisons to Experimental Results," *IEEE Transactions on Microwave Theory and Techniques*, Vol. 40, no. 6, p. 1279, June 1992.